Insights of fibroblast growth factor receptor 3 aberrations in pan-cancer and their roles in potential clinical treatment

Juanni Li[1], Kuan Hu[2], Jinzhou Huang[3], Lei Zhou[4], Yuanliang Yan[5,6], Zhijie Xu[1]

[1]Department of Pathology, Xiangya Hospital, Central South University, Changsha 410008, Hunan, China
[2]Department of Hepatobiliary Surgery, Xiangya Hospital, Central South University, Changsha 410008, Hunan, China
[3]Department of Oncology, Mayo Clinic, Rochester, MN 55905, USA
[4]Department of Anesthesiology, Third Xiangya Hospital of Central South University, Changsha 410008, Hunan, China
[5]Department of Pharmacy, Xiangya Hospital, Central South University, Changsha 410008, Hunan, China
[6]National Clinical Research Center for Geriatric Disorders, Xiangya Hospital, Central South University, Changsha 410008, Hunan, China

Correspondence to: Yuanliang Yan; **email:** yanyuanliang@csu.edu.cn

ABSTRACT

Fibroblast growth factor receptor 3 (FGFR3) alters frequently across various cancer types and is a common therapeutic target in bladder urothelial carcinoma (BLCA) with FGFR3 variants. Although emerging evidence supports the role of FGFR3 in individual cancer types, no pan-cancer analysis is available. In this work, we used the open comprehensive datasets, covering a total of 10,953 patients with 10,967 samples across 32 TCGA cancer types, to identify the full alteration spectrum of FGFR3. FGFR3 abnormal expression, methylation patterns, alteration frequency, mutation location distribution, functional impact, and prognostic implications differed greatly from cancer to cancer. The overall alteration frequency of FGFR3 was relatively low in all cancers. Targetable mutations were mainly detected in BLCA, and S249C, Y373C, G370C, and R248C were hotspot mutations that could be targeted by an FDA approved erdafitinib. Genetic fusions were mainly observed in glioma, followed by BLCA. FGFR3-TACC3 was the most common fusion type which was proposed as novel therapeutic targets in glioma and was targetable with erdafitinib in BLCA. Lung adenocarcinoma (LUAD) and lung squamous cell carcinoma (LUSC) were two lung cancer subtypes, FGFR3 fusion and hotspot mutation like S249C were observed more commonly in LUSC but not in LUAD. DNA methylation was correlated with the expression of FGFR3 and its downstream genes in some tumors. FGFG3 abnormal expression and alterations exhibited clinical correlations with patient prognosis in several tumors. This work exhibited the full alteration spectrum of FGFR3 and indicated several new clues for their application as potential therapeutic targets and prognostic indicators.

INTRODUCTION

The family of fibroblast growth factor receptor (FGFR) comprises four receptor tyrosine kinases (FGFR1, FGFR2, FGFR3, and FGFR4) involved in several critical cellular processes, such as angiogenesis, proliferation, differentiation, and metabolism [1–5]. *FGFR3* is highly expressed in osteoblasts and chondrocytes, and has classically been known to play critical roles in osteogenesis, development, and bone maintenance [6, 7]. Additionally, FGFR3 signaling has been reported to overlap with several known oncogenic pathways such as RAS/EGFR/ERK/PI3K/AKT pathway and has been implicated in epithelial-mesenchymal transition (EMT) in some tumors [8, 9].

In recent years, along with improvements in clinical genetic testing techniques in oncology, more *FGFR3*

gene alterations are discovered and implicated in a wide range of cancers [10–12]. The most common *FGFR3* mutation type detected in tumors is S249C, and the mutagenic mechanism is mediated by catalyzing polypeptide-like (APOBEC) through an apoprotein B mRNA editing enzyme [13]. More recently, erdafitinib, a pan-FGFR targeted inhibitor, was approved by the FDA in April 2019 for advanced urothelial carcinoma with FGFR3 hotspot mutation like S249C as the first molecularly targeted therapy [14–16]. However, it should be noted that not all FGFR3 mutations confer sensitivity to FGFR inhibitors. For example, V555M mutation which is detected in multiple myeloma confers resistance to FGFR3 inhibitors through the steric hindrance of the kinase-inhibitor interaction [17]. Moreover, recently, gene fusions involving FGFR3 have been observed in some cancer types, and glioma harbors the highest FGFR3 fusion rate. FGFR3 -TACC3 is the most identified fusion type, followed by fusions containing BICC1, TACC2, and NPM1 [18, 19]. This fusion type was reported to be able to confer constitutive kinase activity of FGFR3 and promotion of cell transformation and proliferation [20, 21]. These FGFR3 alterations are identified as the oncogenic drivers and are also considered to be potential therapeutic targets. Nowadays, multiple FGFR inhibitors are in the pipeline, further FDA approval is possible, and it is highly likely their application in targeted treatment will extend to other tumor types.

As previous studies on FGFR3 genetic alterations in cancer are limited to the individual cancer types and/or to the insufficient sample sizes, a comprehensive analysis and view across various tumor types of TCGA to investigate their significance have not been explored. In this work, we analyzed the large datasets from TCGA and fill this vacancy in a comprehensive way. We first systematically profiled FGFR3 expression, methylation, genetic alterations, and their clinical and therapeutic implications across 32 TCGA cancer types covering 10,967 tumor samples. Additionally, the survival association between FGFR3 aberration patterns and prognosis in distinct cancer types was conducted to explore its potential therapeutic implication. Conclusively, our analysis results highlight the important role of FGFR3 in tumorigenesis and provide potential and promising therapeutic targets across different cancers.

RESULTS

Expression and methylation level of FGFR3 in different cancer types

FGFR3 abnormal expression has been observed in various cancer types [22, 23]. In this work, we provided a more comprehensive analysis of FGFR3 expression. First of all, we explored the expression pattern of FGFR3 among different types of normal tissues by the GTEx portal. FGFR3 expression exhibited a broad spectrum across different tissues. FGFR3 showed the highest expression in the skin and almost no expression in the EBV-transformed lymphocytes (Supplementary Figure 1). Next, FGFR3 expression was compared across 32 TCGA cancer types (Supplementary Table 1). As shown in Supplementary Figure 2A, FGFR3 expression across different cancers was dramatically different, indicating that high FGFR3-expressing cancers may have some genetic features that lead to the increased FGFR3 expression. According to the interquartile range, FGFR3 expression spread varied in several cancers more than others, for example, skin cutaneous melanoma (SKCM) had a wide spread while testicular germ cell tumors (TGCT) had a narrow spread, which may be on account of some cancer types including several subtypes and thus having more genetic diversity (Supplementary Figure 2A). Moreover, we evaluated the expression difference of FGFR3 between tumors and the corresponding normal tissues profiled in TCGA. As shown in Figure 1A, significantly differential expression of FGFR3 was observed in 16 tumor types, with 10 tumor types upregulated [breast invasive carcinoma (BRCA), cervical squamous cell carcinoma and endocervical adenocarcinoma (CESC), cholangiocarcinoma (CHOL), esophageal carcinoma (ESCA), head and neck squamous cell carcinoma (HNSC-HPV), LICH, LUSC, SKCM, stomach adenocarcinoma (STAD), thyroid carcinoma (THCA)] and 6 tumor types downregulated [colon adeno-carcinoma (COAD), GBM, kidney chromophobe (KICH), kidney renal clear cell carcinoma (KIRC), kidney renal papillary cell carcinoma (KIRP), LUAD]. After adding GTEx normal tissues as control, we further compared FGFR3 expression difference between the normal tissues and tumors of adrenocortical carcinoma (ACC), lymphoid neoplasm diffuse large B-cell lymphoma (DLBC), acute myeloid leukemia (LAML), LGG, ovarian serous cysta-denocarcinoma (OV), sarcoma (SARC), TGCT, thymoma (THYM), and uterine carcinosarcoma (UCS). Upregulated expression of FGFR3 was observed in 4 cancer types (OV, TGCT, THYM, and UCS) and downregulated expression of FGFR3 was observed in 2 cancer types (LAML and LGG) (Figure 1B, Supplementary Figure 3A). Furthermore, we explored the correlation between FGFR3 expression and the tumor pathological stages by the GEPIA2 approach. It was found that FGFR3 expression was correlated with tumor pathological stages in several cancer types, including BLCA, KICH, KIRC, LUAD, SKCM, and uterine corpus endometrial carcinoma (UCEC) (Figure 1C, all

Figure 1. Fibroblast growth factor receptor 3 (FGFR3) mRNA expression and DNA methylation in The Cancer Genome Atlas (TCGA) tumor tissues. (**A**) The mRNA expression of FGFR3 in different cancers or specific cancer subtypes from TIMER2. The log2 [TPM (Transcripts per million)] was applied for log-scale. (**B**) For LAML, LGG, OV, TGCT, THYM, and UCS from the TCGA project, their corresponding normal tissues of the GTEx database were included as controls based on the GEPIA2 portal. The log2 (TPM +1) was applied for log-scale. (**C**) FGFR3 mRNA expression levels were analyzed by the main pathological stages of BLCA, KICH, KIRC, LUAD, SKCM, and UCEC. The log2 (TPM +1) was applied for log-scale. (**D**) Bubble map showing the differential methylation of FGFR3 and its downstream genes between tumors and matched normal samples. Blue dots, downregulated methylation in tumors. Red dots, upregulated methylation in tumors. (**E**) Bubble map depicting the relative methylation and expression differences of FGFR3 and its downstream genes between tumors and matched normal samples by size and color, respectively. Blue dots, upregulation in methylation level but downregulation in expression level. Red dots, upregulation in both methylation and expression levels of indicated genes. *$P < 0.05$; **$P < 0.01$; ***$P < 0.001$.

P < 0.05). However, no correlation was found in the remaining cancer types (Supplementary Figure 3B–3F, all *P* > 0.05).

DNA methylation was reported to be strongly associated with the change of gene expression in tumors [24, 25]. Therefore, we applied the GSCALite approach to explore the methylation status of FGFR3 and its downstream genes in various cancer types of TCGA. As shown in Figure 1D, up-regulated methylation of FGFR3 was observed in KIRC, KIRP, HNSC, UCEC, and LUAD, while down-regulated methylation of FGFR3 was found in BLCA, BRCA, and LUSC. In addition, the expression of FGFR3 and its downstream genes were found to be most negatively correlated with FGFR3 methylation status, with only a few positive correlations (Figure 1D).

FGFR3 somatic mutation patterns in different cancer types

The total mutation frequency of FGFR3 was 2.13% for all cancer samples (234/10,967) across various cancer types of TCGA. The tumor sample number from different cancer types varied from 36 (CHOL) to 1,084 (BRCA) (Supplementary Table 2). Those cancer types with too few samples such as CHOL might not represent the full landscape of FGFR3 mutation status. Moreover, as shown in Figure 2A, BLCA (18.5%), SKCM (4.9%), and UCEC (4.5%) were the most common cancer types with FGFR3 mutations. On the contrary, almost no FGFR3 mutations were observed in ACC, CHOL, DLBC, KICH, pheochromocytoma and paraganglioma (PCPG), TGCT, THCA, THYM, and uveal Melanoma (UVM).

We observed 234 FGFR3 somatic mutations across 32 TCGA cancers, among these mutations, 42 FGFR3 mutations belonged to fusion. As shown in Figure 3, fusion transcripts of FGFR3 were observed in BLCA (8), LUSC (7), CESC (6), LGG (5), GBM (3), ESCA (2), KIRP (2), liver hepatocellular carcinoma (LIHC) (2), HNSC (2), STAD (1), prostate adenocarcinoma (PRAD) (1), OV (1), SKCM (1), ACC (1). The highest number of fusion transcripts was found in BLCA (eight FGFR3_TACC3), followed by LUSC (six FGFR3_TACC3, one TACC3_FGFR3), CESC (five FGFR3_TACC3, one TACC3_FGFR3), and LGG (two FGFR3_TACC3, one TACC3_FGFR3, one FGFR3_ELAVL3, one FGFR3_FBXO28). FGFR3_TACC3 was the most common fusion transcripts of FGFR3 (32/42) and distributed in different cancer types [BLCA (8), LUSC (6), CESC (5), ESCA (2), LGG (2), HNSC (2), KIRP (2), LIHC (2), GBM (1), STAD (1), ACC (1)]. TACC3 is a tumor-associated protein that has been found to play critical

roles in the development of various cancer types, such as ovarian cancer, hepatocellular carcinoma, glioblastoma, and so on. It was also involved in several crucial cellular events, like cell differentiation, growth, transcriptional regulation, and the regulation of centrosome and microtubule [26]. Most fusion transcripts of FGFR3 were classified as the in-frame, while three FGFR3_TACC3 (one BLCA, one LUSC, one LIHC) were classified as the out-of-frame.

FGFR3 was found to have four functional domains based on the Pfam database, containing the PKinase_Tyr domain (472–748 aa), I-set domain (260–356 aa), I-set domain (166–245 aa), and ig domain (54–110 aa). In this analysis, 234 FGFR3 mutations were detected in various cancer types of TCGA and distributed across different FGFR3 functional domains. As shown in Figure 2B, the other domain whose function was barely known was the most frequently mutated domain of FGFR3 (100 samples), followed by the Pkinase_Tyr domain (54 samples), the I-set (260–356 aa, 20 samples), the I-set (166–245 aa, 9 samples), and the ig domain (9 samples). Moreover, the location distribution of FGFR3 mutations differed greatly across different TCGA cancers. Mutations in UCEC, SKCM, colon adenocarcinoma/rectum adenocarcinoma (COADREAD), STAD, and KIRP were most commonly distributed in the Pkinase_Tyr domain. Mutations in BLCA and HNSC were primarily located in the other domain and amounted to around two-thirds of all FGFR3 mutations. Mutations in LGG and CESC were mainly fusion, especially for CESC, fusion was the only mutation type in this cancer type. In LUSC, fusion and mutations in the other domain were equally common (Figure 2B and Supplementary Table 3).

The 234 FGFR3 mutations mentioned above were classified into three categories based on mutation functional impact on FGFR3 protein coding, including missense mutations (177 samples), fusion (42 samples), and truncating mutations (15 samples). The most common mutation positions of FGFR3 were S249C (41 samples) and Y373C (11 samples), both of which were located in the other domain. Mutations at S249C were most observed in BLCA samples which were amounted to nearly three-quarters of all mutations in this position (32/41). The S249C was an FGFR3 hotspot mutation and known to be oncogenic. Patients with metastatic urothelial tumor carrying S249C mutation could be treated with the pan-FGFR targeted inhibitor, erdafitinib, which was approved by Food and Drug Administration (FDA) [27, 28]. The other cancer types carrying S249C mutation were HNSC (4 samples), LUSC (4 samples), and KIRP (one sample). However, different from that in BLCA, the clinical utility of targeted drugs in these three cancer types with S249C

mutation was still unknown. Similarly, BLCA harbored the largest proportion of mutations at Y373C (8/11), followed by KIRP (two samples) and UCEC (one sample). BLCA with a mutation at this position could be also treated with the FDA-approved erdafitinib (Supplementary Figure 4A) [27, 28]. Moreover, as shown in Figure 2A and Supplementary Figure 4B, BLCA had the highest frequency of FGFR3 mutational alterations. S249C was most common among BLCA mutation samples (32 samples), followed by Y373C (8 samples), G370C (5 samples), and R248C (3 samples). All these four mutation positions of FGFR3 were oncogenic and were FDA recognized biomarker predictive of response to an FDA-approved drug, such as erdafitinib [27, 28]. For mutations at K650E (two samples), S371C (two samples), and G380R (two samples) in BLCA, there was promising clinical

evidence that supported these mutation positions as being predictive of response to pan-FGFR-targeted inhibitors such as Debio1347, BGJ398, AZD4547, and erdafitinib [27, 29–33]. Furthermore, in UCEC, the most mutated positions were in the Pkinase_Tyr domain. Mutation at Y373H in UCEC was considered likely oncogenic, and several laboratory data suggested that tumor cells with Y373H mutation may be sensitive to some selective FGFR-targeted inhibitors (Supplementary Figure 4C) [28, 34–36].

The 234 FGFR3 mutations were divided into five classes based on their predictive significance and oncogenic effect, including unknown (113 mutations), oncogenic (94 mutations), likely oncogenic (22 mutations), predicted oncogenic (1 mutation), and likely neutral (4 mutations). As shown in Figure 4A, nearly
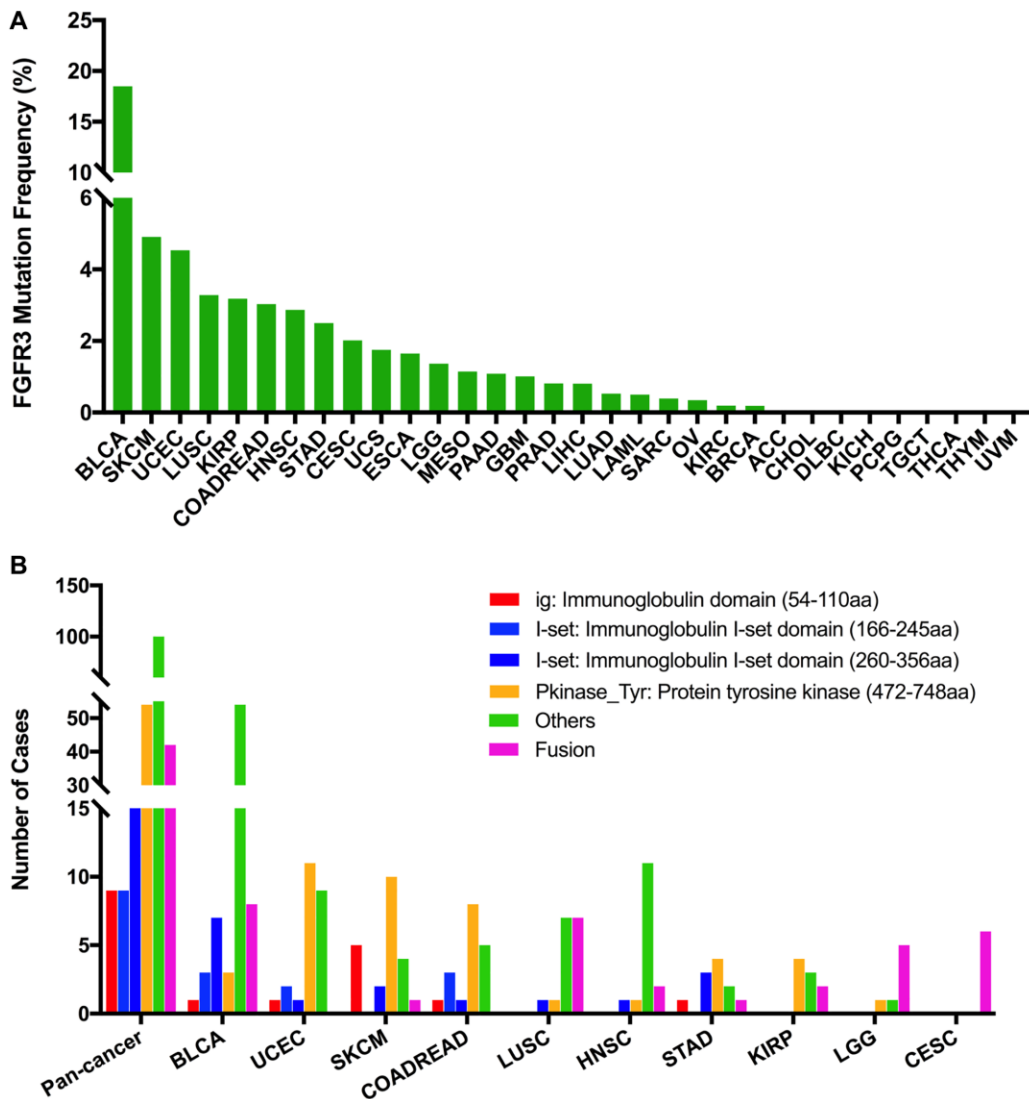
Figure 2. FGFR3 mutation distribution in different cancer types of TCGA and protein functional domains. (**A**) The mutation frequency of FGFR3 across various tumor types. (**B**) FGFR3 mutation distribution in different protein functional domains in all and top ten tumor types. Abbreviation: aa: amino acid.

half of FGFR3 somatic mutations were distributed in the unknown class, indicating that more research needs to be conducted to explore the role of these mutations. However, mutations that were distributed in the functional classes took up a major portion of FGFR3 mutations in several cancers such as BLCA, LUSC, HNSC, KIRP, and CESC. In BLCA and LUSC, about two-thirds of mutations belonged to the oncogenic class (53/76, 11/16, respectively), and the other mutation that was distributed in the functional class was likely oncogenic (nine mutations, one mutation, respectively). In CESC, all somatic mutations of FGFR3 belonged to oncogenic (Figure 4B).

Then we used the cBioPortal approach to analyze the clinical targeted therapy application potential of FGFR3 somatic mutations. The 234 FGFR3 mutations were classified as five levels which were defined by OncoKB [37], containing level NA (118 mutations), level 4 (four mutations), level 3B (50 mutations), level 3A (six mutations), and level 1 (56 mutations). Approximately half of the FGFR3 mutations were classified as level NA which represented no targeted therapy implication,

indicating that more work was needed to improve the status of the current targeted treatment (Figure 5A). All level 1 mutations were found in BLCA, which accounted for nearly two-thirds of FGFR3 mutations. Most of these level 1 mutations were S249C, and the remaining mutations were Y373C, G370C, and R248C. BLCA patients with these level 1 mutations were suitable for targeted treatment with an FDA-approved medicine [16]. Meanwhile, there were six mutations in BLCA that belonged to level 3A, which represented that there was promising clinical evidence that supported these level 3A mutations as being predictive of response to targeted therapy. Furthermore, level 3B mutations were distributed in several cancer types such as LUSC, HNSC, KIRP, LGG, and CESC (Figure 5B).

FGFR3 CNVs across cancer types

Here, we explored the CNVs of FGFR3 in different cancer types. The overall CNV frequency of FGFR3 was about 34.5% (3784/10,967 samples). The most common CNV type of FGFR3 was shallow deletion (2625 samples), then gain (1000 samples), amplification
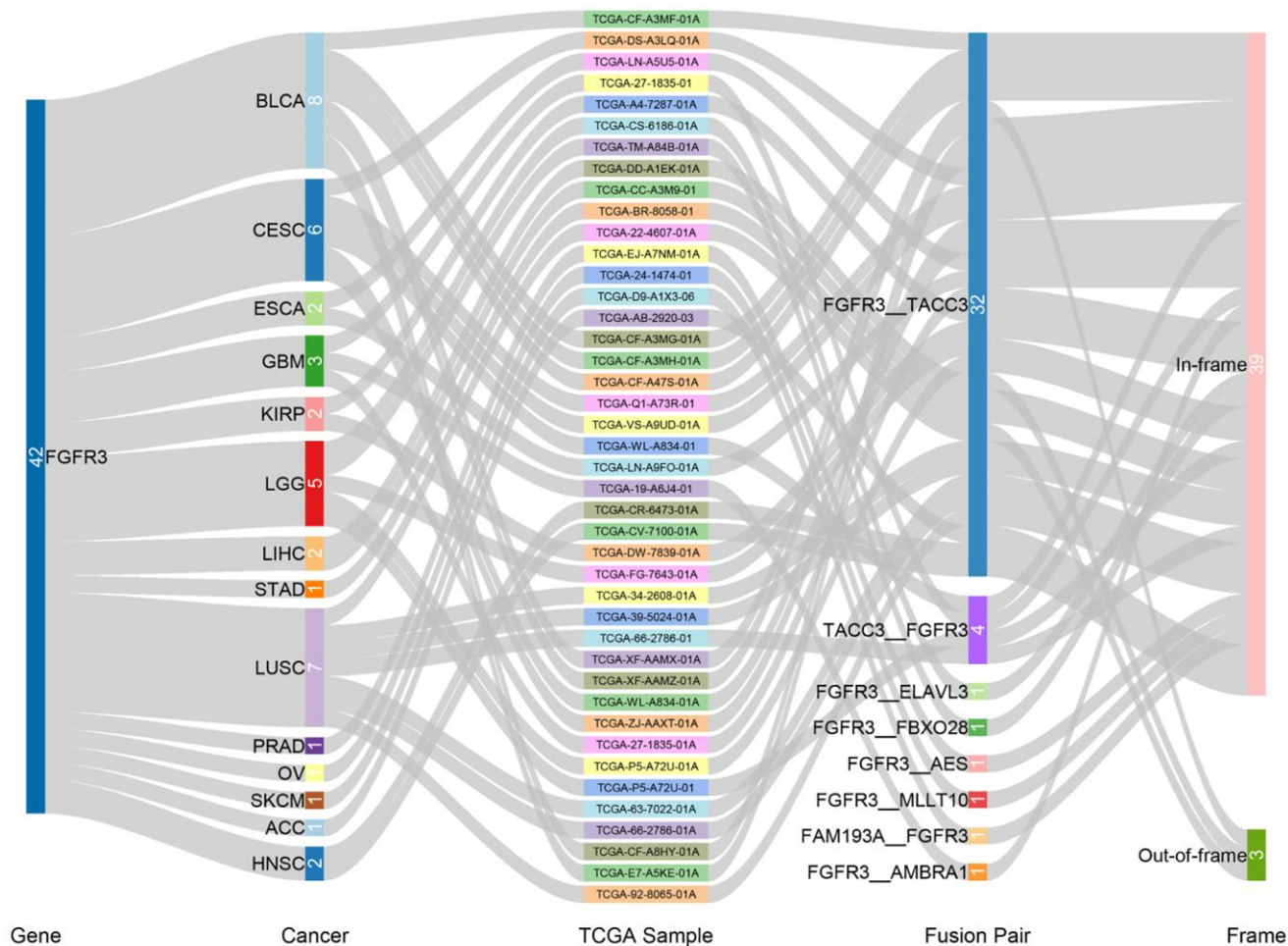

Figure 3. Fusion gene of FGFR3 across 32 TCGA tumor types.

(120 samples), and deep deletion (39 samples). Most of the amplification were mainly detected in UCS, OV, and BLCA, while most of the deep deletion was found in ESCA, HNSC, CESC, and BRCA (Figure 6A). The most common cancer types with FGFR3 CNVs were UCS (78.9%), LUSC (69.2%), ESCA (68.7%), OV (66.5%), and TGCT (65.1%). On the contrary, THCA (1.6%), LAML (3.0%), THYM (6.5%), DLBC (8.3%), and PCPG (9.0%) had very low CNV frequency of FGFR3 (Figure 6A). Next, we analyzed the correlation between FGFR3 CNVS and its mRNA expression. As shown in Supplementary Figure 2B, there was no significate correlation was found between FGFR3 CNVs and its mRNA expression across different cancer types ($r = 0.0127$, $p = 0.2052$), suggesting that some other genetic alterations may lead to FGFR3 expression. Mesothelioma (MESO) and DLBC had a relatively high proportion of shallow deletion and were also the tumor type with relatively lower FGFR3 expression. However, KICH and ACC who harbored a relatively high proportion of gain showed a lower expression of FGFR3. Similarly, TGCT, HNSC, CESC, and LUSC
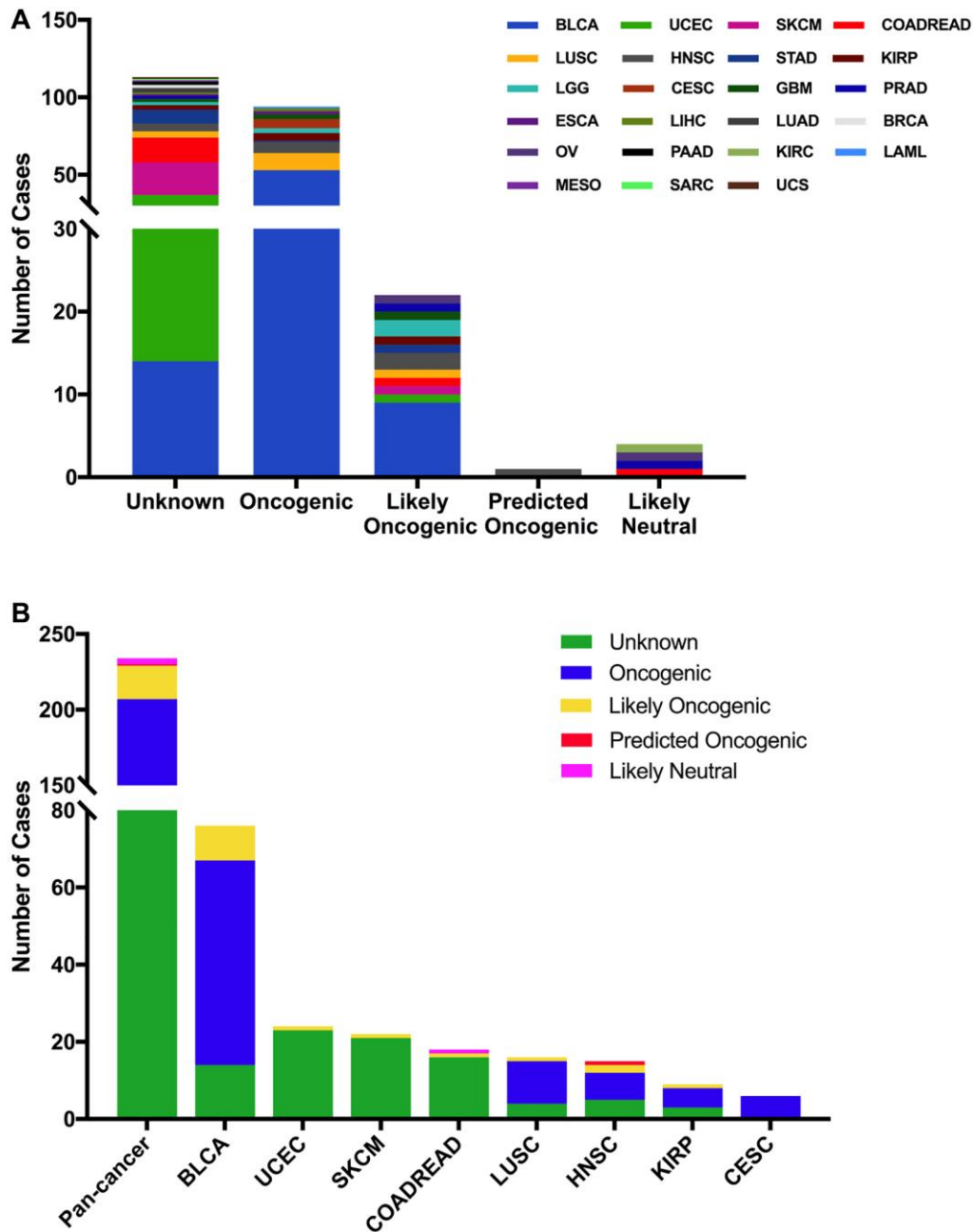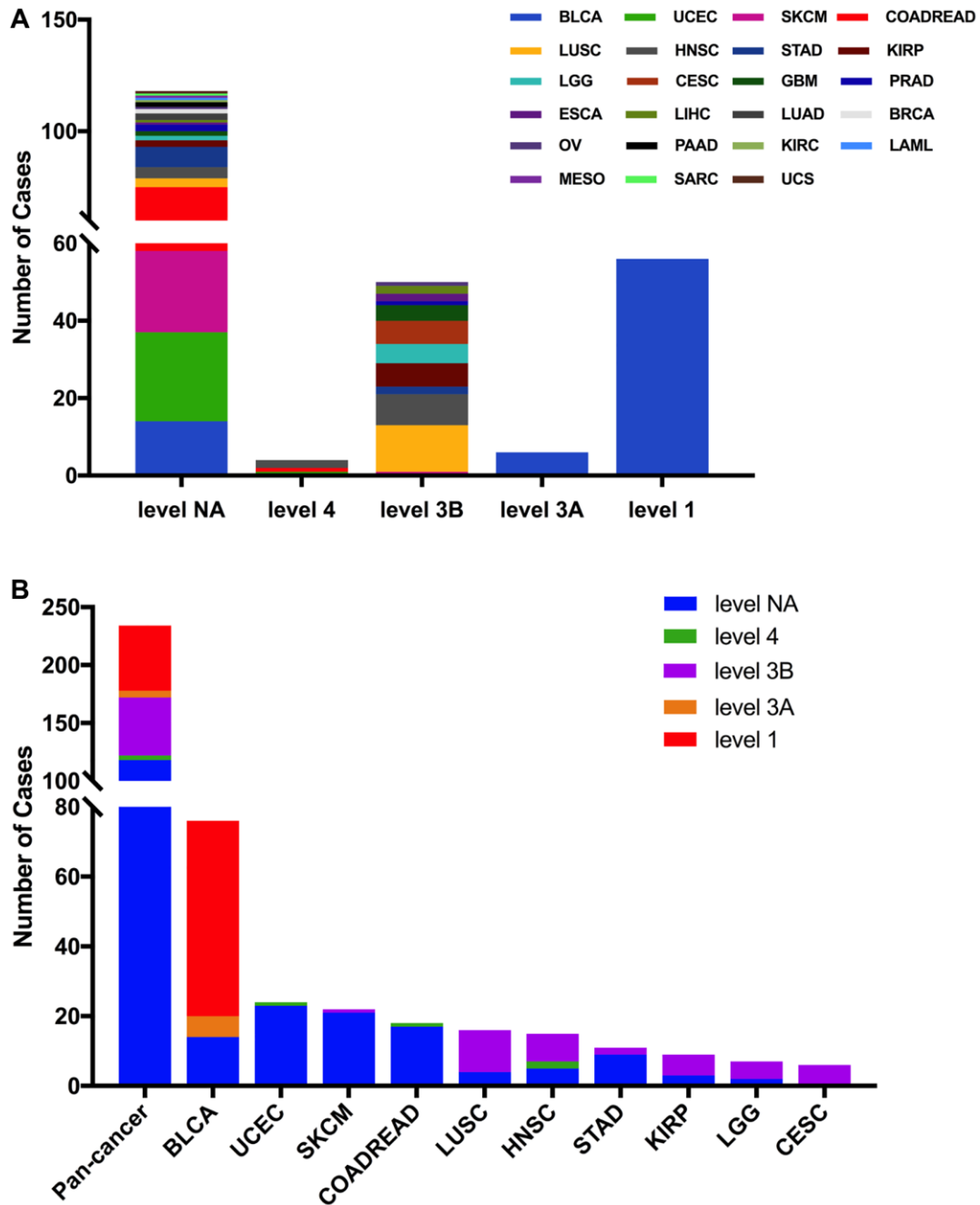

Figure 4. FGFR3 mutation classification based on the functional impact on protein coding. (**A**) FGFR3 mutations were categorized according to the functional impacts on all tumors together. (**B**) Functional impact category distribution of FGFR3 mutations in pan-cancer and the top eight tumor types.

had a higher proportion of shallow deletion but was the cancer types with relatively higher expression of FGFR3 (Figure 6A, Supplementary Figure 2A). Furthermore, as shown in Figure 6B, among the 234 samples with FGFR3 mutations described above, 81 samples had FGFR3 CNVs at the same time, of which 32 samples had shallow deletions, 26 samples had gains, 22 samples had amplifications, and one sample had deep deletion. BLCA harbored the highest number of amplification and gain across different cancer types.

LUSC and BLCA had the same number and also the highest number of shallow deletions (Figure 6B, Supplementary Table 2).

Combined FGFR3 alterations (CNVs and mutation) across cancer types

Here, we further analyzed the combined alterations of FGFR3 including mutation and CNVs across different cancer types. The overall alteration frequency of


Figure 5. FGFR3 mutation classification according to clinical therapeutic implications. (**A**) FGFR3 mutations were classified according to the therapeutic implications defined by OncoKB among all tumors together. (**B**) Therapeutic implications class distribution of FGFR3 mutations in pan-cancer and the top ten tumor types.

FGFR3 was about 3.2% (detected in 351 of 10,967 samples). As shown in Figure 7A, FGFR3 alterations across different cancer types were quite different. BLCA (18.73%) harbored the most frequency of FGFR3 alterations in which mutation took up a major portion. Other cancers that had dominant FGFR3 mutations but were at relative lower alteration frequency contained UCEC (6.81%), SKCM (5.18%), STAD (3.64%), HNSC (3.63%), COADREAD (3.37%), KIRP (2.47%) and MESO (1.38%). UCS (15.79%) had the second most frequency of FGFR3 alterations with dominant FGFR3 amplification. Similar alteration pattern which was dominant amplification but relatively few mutation was observed in some cancer types such

as OV, ACC, CHOL, pancreatic adenocarcinoma (PAAD), GBM, SARC (4.3 vs 0.2%, 3.3 vs 0.0%, 2.8 vs 0.0%, 2.2 vs 0.5%, 1.4 vs 0.5%, 1.6 vs 0.4%, respectively). Fusion was more common in BLCA (1.7%), CESC (1.35%), LUSC (1.23%), and ESCA (1.1%). Deep deletion was mainly distributed in ESCA (2.2%), CESC (1.35%), HNSC (0.96%), LUSC (0.82%), and BRCA (0.74%). Some tumors harbored neither mutations nor CNVs of FGFR3 such as DLBC, KICH, TGCT, and UVM.

Next, we found that mutation location and CNV occurrence of FGFR3 were correlated. As we mentioned above, 234 FGFR3 mutations across 32
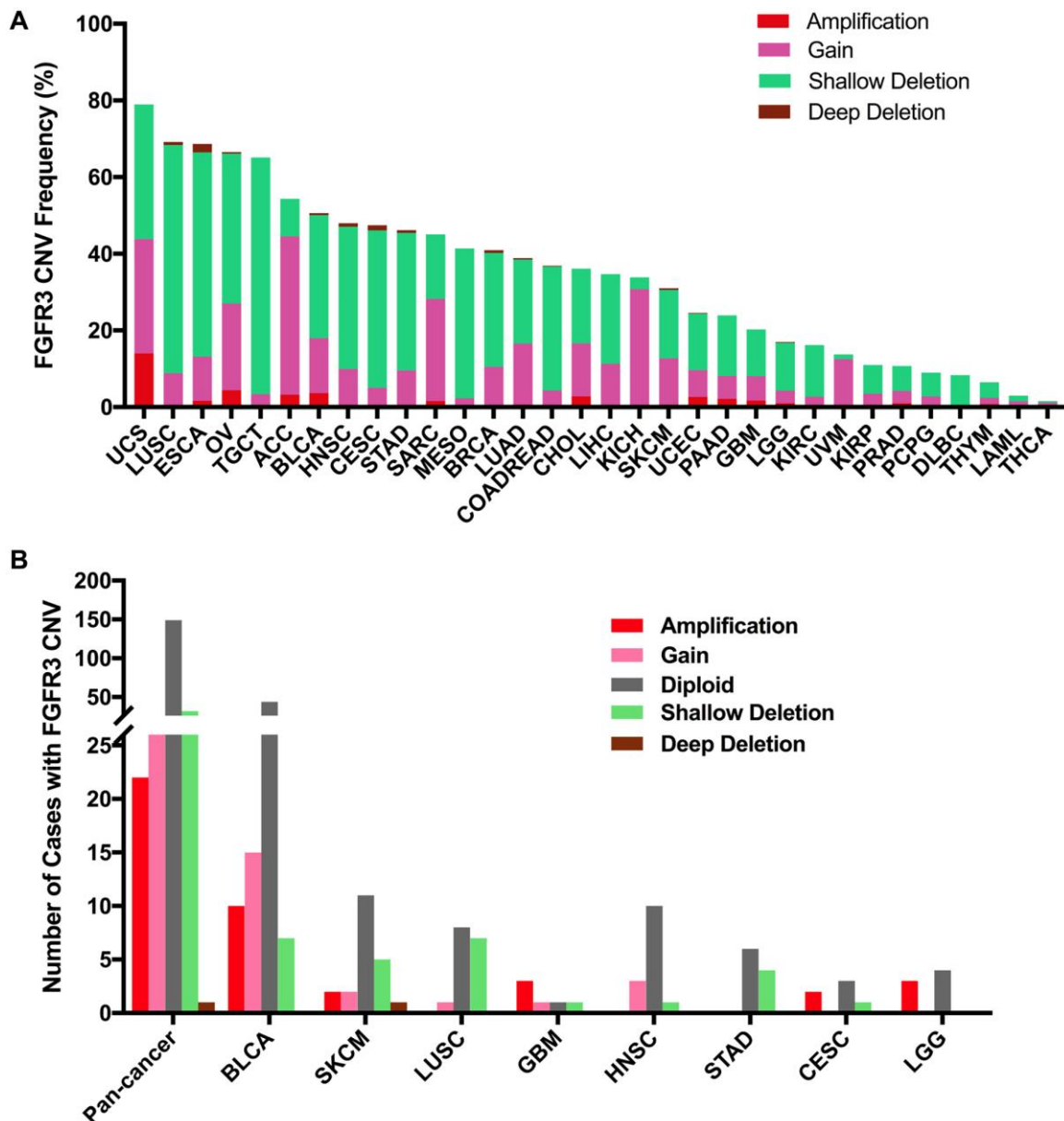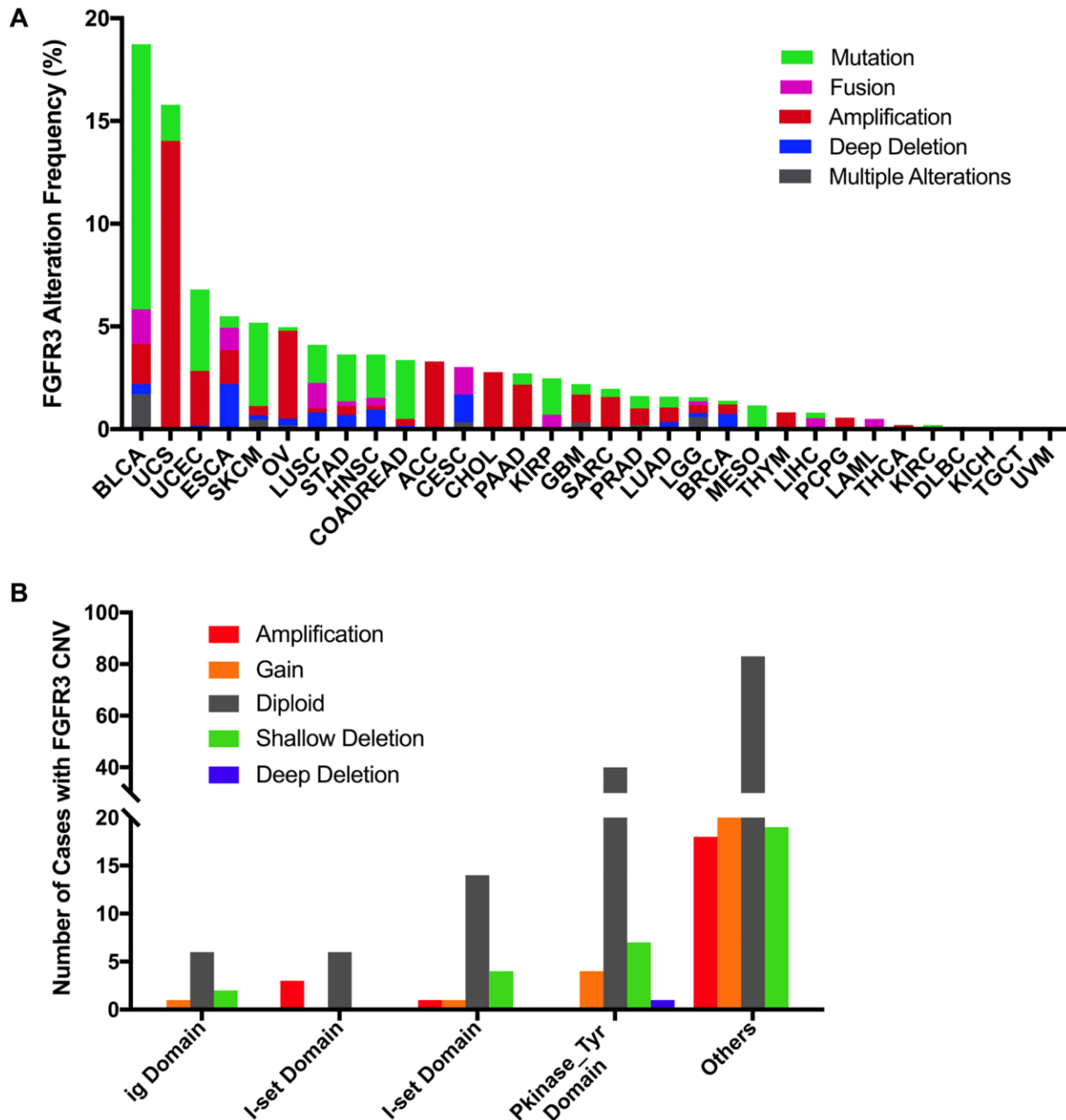

Figure 6. Pan-cancer analysis of FGFR3 Copy Number Variant (CNV). (**A**) The CNV frequency of FGFR3 across various tumor types. (**B**) FGFR3 CNV distribution in pan-cancer and the top eight tumors for the cases with FGFR3 mutations simultaneously.

TCGA cancers were detected in this analysis. Interestingly, we further found that nearly two-fifths of FGFR3 mutations in the other function-unknown domain were accompanied by shallow deletion, gain, and amplification (57 of 140 mutations). Approximately one-third of FGFR3 mutations in the ig domain, I-set domain (166–245 aa), or I-set domain (260–356 aa) harbored shallow deletion, gain, and amplification (3 of 9 mutations, 3 of 9 mutations, 6 of 20 mutations, respectively). About one-fifth of FGFR3 mutations in the Pkinase_Tyr domain were accompanied by deep

deletion, shallow deletion, gain, and amplification (12 of 52 mutations) (Figure 7B).

FGFR3 alterations and patient survival in different cancer types

In order to evaluate the clinical value of FGFR3 expression, the correlation between the mRNA expression of FGFR3 and patient overall survival (OS) and recurrence-free survival (RFS) was analyzed across different cancer types. As shown in Figure 8A,

Figure 7. Pan-cancer analysis of FGFR3 alterations and distribution. (**A**) The alteration (mutation and CNVs) frequency of FGFR3 across various tumor types. (**B**) The distribution of CNV cases along with mutations located in protein functional domains.

increased mRNA expression of FGFR3 was correlated with poor patient OS in COADREAD and UCEC. However, the survival results for patients with CESC, HNSC, KIRC, and STAD showed that high mRNA expression of FGFR3 was correlated with better OS. In addition, survival correlation analysis between mRNA expression of FGFR3 and patient RFS across different tumors exhibited that increased mRNA expression of FGFR3 was correlated with poor RFS in ESCC, KIRP, and UCEC, while high mRNA expression of FGFR3 was correlated with better RFS in HNSC, LUSC, and THCA (Supplementary Figure 5). Meanwhile, we further conducted the survival association analysis regarding alteration status across different cancers to explore the clinical value of the FGFR3 alterations. As shown in Figure 8B, FGFR3 alterations were correlated with poor prognosis in SARC, while FGFR3 alterations were correlated with better survival in UCS and BLCA. These opposite survival results may be on account of insufficient sample sizes and different genetic backgrounds.
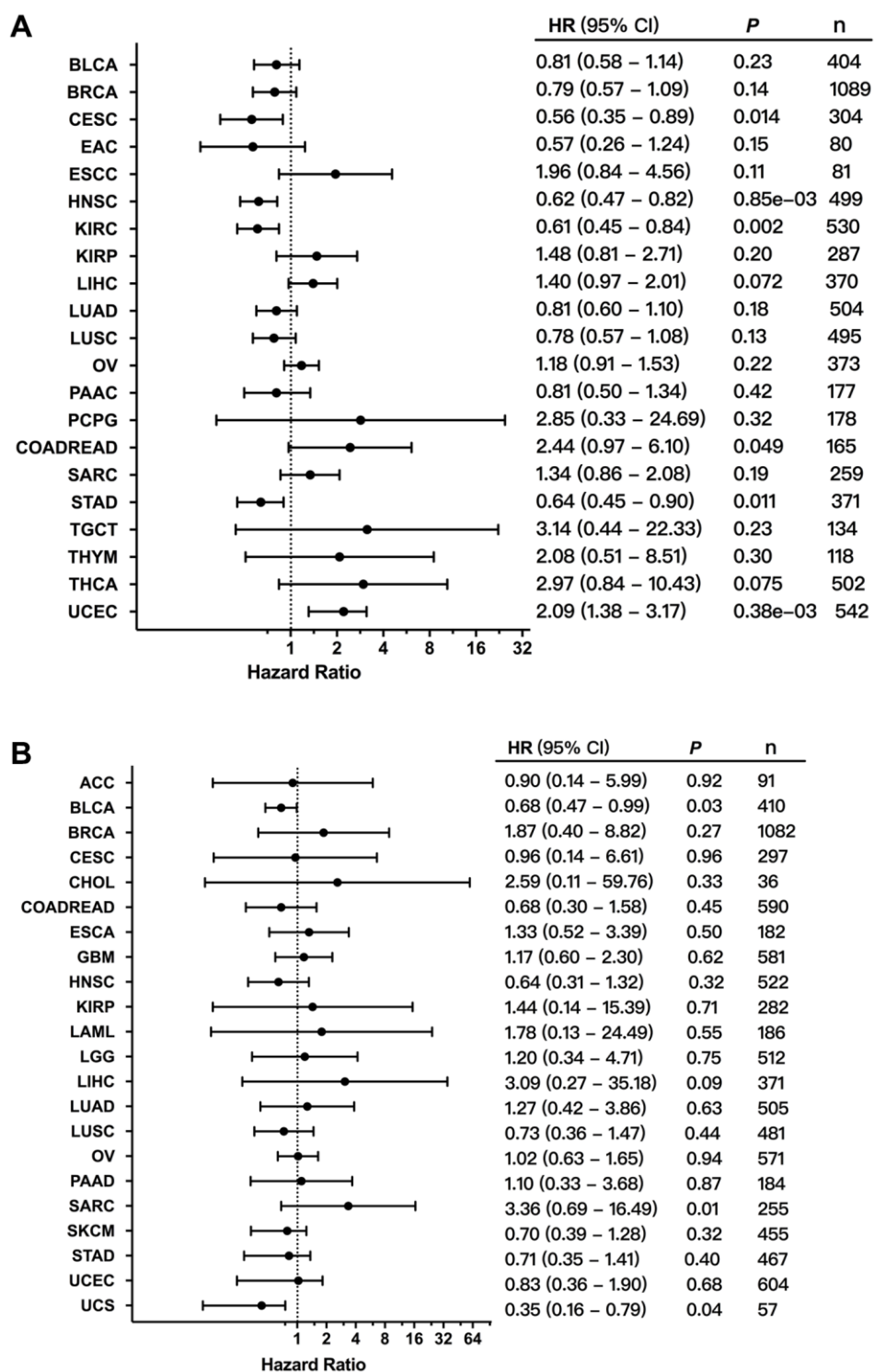
DISCUSSION

In this study, the characteristics of FGFR3 across 32 TCGA cancer types were profiled, which were of critical therapeutic and clinical significance. The analysis results showed that FGFR3 expression, methylation, and alteration varied greatly from cancer to cancer. BLCA and UCS had the most frequency of FGFR3 alterations among different cancers. In BLCA, the most common alteration type was the mutation, which was mainly located in the other function-unknown domain, then in the I-set domain. S249C was the most common mutation position in BLCA, followed by the other three mutation sites including Y373C, G370C, R248C. These four mutation sites were all FDA-recognized biomarker predictive of response to an FDA-approved drug, such as erdafitinib [27, 28]. Fusion was also very common in BLCA, FGFR3-TACC3 was the most common fusion type. Patients with metastatic urothelial tumors carrying FGFR3-TACC3 fusion could be also treated with the pan-FGFR targeted inhibitor, erdafitinib [28]. In UCS, amplification was the most common alteration type but mutation was relatively less. The survival association analysis showed that for patients with UCS, FGFR3 alterations were associated with longer overall survival time. In several cancer types amplification accounted for a major proportion of FGFR3 alterations such as OV, ACC, CHOL, PAAD, GBM, and SARC. OV and CHOL harbored high expression of FGFR3, and GBM harbored low expression of FGFR3, however, there was no survival correlation was found between FGFR3 expression and prognosis in these tumors. Some cancer types had dominant mutations but rare CNVs of FGFR3 such as

SKCM, COADREAD, KIRP, and MESO. In SKCM, COADREAD, and MESO, most mutations belonged to unknown categories and level NA, and more efforts were needed to figure out their function thus contribute to the clinical treatment. While in KIRP, most mutations were oncogenic and likely oncogenic and belonged to level 3B which was classified by the clinical targeted therapy application potential of FGFR3 somatic mutations. Moreover, ESCA and CESC had the most frequency of deep deletion of FGFR3, but these two cancer types both had high FGFR3 expression, suggesting that some other genetic features may affect the expression of FGFR3. Furthermore, the relatively high frequency of FGFR3 fusion was mainly distributed in BLCA, CESC, LUSC, and ESCA. Several fusion types were detected such as FGFR3-TACC3 and TACC3-FGFR3, TACC3 was the most common partner gene of FGFR3.

The therapeutic landscape of BLCA has dramatically changed in recent years: standard therapy remains platinum chemotherapy, followed by immune checkpoint inhibitors as second-line or maintenance [38–40]. Nowadays, the emergence of FGFR-targeted inhibitors such as erdafitinib was shifting the treatment paradigm for patients with BLCA harboring FGFR3 genetic alterations [16]. In this analysis, we observed that BLCA had the highest frequency of FGFR3 alterations, and mutation took up a major portion. The most common activating point mutations of FGFR3 observed in BLCA from our analysis were S249C, followed by R248C, Y373C, G370C, which were located in exons 7, 15, 10, and 10, respectively. All these four FGFR3 point mutations were oncogenic and belonged to level 1 which was categorized by the clinical targeted therapy application potential of FGFR3 mutations. In addition to these activating FGFR3 point mutations, gene fusion involving FGFR3 such as FGFR3-TACC3 was also commonly detected in BLCA. Patients with BLCA harboring these FGFR3 hotspot mutations or FGFR3-TACC3 fusion were suitable for targeted treatment with an FDA-approved drug, erdafitinib [16]. Erdafitinib, a tyrosine kinase inhibitor (TKI) of FGFR, was approved by the USA FDA in April 2019 for advanced urothelial carcinoma with actionable FGFR2/FGFR3 alterations as the first molecularly targeted therapy [14, 15]. Then the therascreen FGFR RT-PCR kit developed by Qiagen was also approved by FDA as a companion diagnostic test, which was marking a new era of biomarker-driven drug discovery for BLCA. Moreover, erdafitinib was also being explored as a therapy for other FGFR alteration-harboring cancers such as ESCA, CHOL, LIHC, PRAD, and LUSC [16, 41]. In addition to erdafitinib which was for therapy of BLCA with FGFR genetic alterations, other FGFR inhibitors including

infigratinib (BGJ398), pemigatinib, rogaratinib, and debio 1347 have been explored under different clinical trials in recent years, exhibiting encouraging clinical data results for BLCA targeted treatment [33, 42–44]. Furthermore, in this analysis, several less common point mutations such as K650E, S371C, and G380R were also observed in BLCA. There was promising clinical evidence that supported these mutation positions as being predictive of response to pan-FGFR-targeted inhibitors such as Debio1347 and BGJ398 [29, 32, 33].

A

	HR (95% CI)	P	n
BLCA	0.81 (0.58 – 1.14)	0.23	404
BRCA	0.79 (0.57 – 1.09)	0.14	1089
CESC	0.56 (0.35 – 0.89)	0.014	304
EAC	0.57 (0.26 – 1.24)	0.15	80
ESCC	1.96 (0.84 – 4.56)	0.11	81
HNSC	0.62 (0.47 – 0.82)	0.85e–03	499
KIRC	0.61 (0.45 – 0.84)	0.002	530
KIRP	1.48 (0.81 – 2.71)	0.20	287
LIHC	1.40 (0.97 – 2.01)	0.072	370
LUAD	0.81 (0.60 – 1.10)	0.18	504
LUSC	0.78 (0.57 – 1.08)	0.13	495
OV	1.18 (0.91 – 1.53)	0.22	373
PAAC	0.81 (0.50 – 1.34)	0.42	177
PCPG	2.85 (0.33 – 24.69)	0.32	178
COADREAD	2.44 (0.97 – 6.10)	0.049	165
SARC	1.34 (0.86 – 2.08)	0.19	259
STAD	0.64 (0.45 – 0.90)	0.011	371
TGCT	3.14 (0.44 – 22.33)	0.23	134
THYM	2.08 (0.51 – 8.51)	0.30	118
THCA	2.97 (0.84 – 10.43)	0.075	502
UCEC	2.09 (1.38 – 3.17)	0.38e–03	542

Hazard Ratio

B

	HR (95% CI)	P	n
ACC	0.90 (0.14 – 5.99)	0.92	91
BLCA	0.68 (0.47 – 0.99)	0.03	410
BRCA	1.87 (0.40 – 8.82)	0.27	1082
CESC	0.96 (0.14 – 6.61)	0.96	297
CHOL	2.59 (0.11 – 59.76)	0.33	36
COADREAD	0.68 (0.30 – 1.58)	0.45	590
ESCA	1.33 (0.52 – 3.39)	0.50	182
GBM	1.17 (0.60 – 2.30)	0.62	581
HNSC	0.64 (0.31 – 1.32)	0.32	522
KIRP	1.44 (0.14 – 15.39)	0.71	282
LAML	1.78 (0.13 – 24.49)	0.55	186
LGG	1.20 (0.34 – 4.71)	0.75	512
LIHC	3.09 (0.27 – 35.18)	0.09	371
LUAD	1.27 (0.42 – 3.86)	0.63	505
LUSC	0.73 (0.36 – 1.47)	0.44	481
OV	1.02 (0.63 – 1.65)	0.94	571
PAAD	1.10 (0.33 – 3.68)	0.87	184
SARC	3.36 (0.69 – 16.49)	0.01	255
SKCM	0.70 (0.39 – 1.28)	0.32	455
STAD	0.71 (0.35 – 1.41)	0.40	467
UCEC	0.83 (0.36 – 1.90)	0.68	604
UCS	0.35 (0.16 – 0.79)	0.04	57

Hazard Ratio

Figure 8. Correlation between the expression and alterations of FGFR3 and patient survival. (**A**) The correlation between FGFR3 expression and overall survival (OS) as exhibited in forest plot based on Kaplan-Meier Plotter. (**B**) The correlation between FGFR3 alterations and OS as exhibited in forest plot based on cBioPortal.

Previous studies reported that FGFR3 genetic fusion was most common in glioma, followed by BLCA. FGFR3 fusion with TACC3 was the classic fusion type that happened in glioma [18]. In this analysis, we found that GBM and LGG had similar mutation rates, and FGFR3 fusion accounted for a major portion. The FGFR3 fusion types observed in glioma (GBM and LGG) in our analysis included FGFR3-TACC3, TACC3-FGFR3, FGFR3-AMBRA1, FGFR3-ELAVL3, FGFR3-FBXO28, and TACC3 was observed to be the most common partner gene of FGFR3 fusion. The first two FGFR3 fusions with TACC3 were oncogenic, and the last three FGFR3 fusion types were likely oncogenic. All of these FGFR3 fusions belonged to level 3B. Patients with glioma harbored FGFR3 fusions were reported to have responded well to FGFR inhibition, and these FGFR3 fusions have been proposed as novel therapeutic targets in glioma [45, 46]. In addition to glioma, FGFR3-TACC3 was also a commonly occurring fusion type in some other cancer types such as BLCA and LUSC. Especially in BLCA, as described above, patients harboring FGFR3-TACC3 could be treated with an FDA-approved drug, erdafitinib [16]. Recent findings revealed that FGFR3-TACC3 could activate oxidative phosphorylation and mitochondrial biogenesis, and engaged oncogenic circuit [47]. More efforts were needed to explore the application of different FGFR inhibitors across various cancers harboring FGFR alterations.

LUAD and LUSC were the two histological types of lung carcinoma [48–50]. Activation of the FGFR family through fusion with various partners has been observed in several cancers, including lung carcinoma. Emerging clinical data showed that these fusions conveyed sensitivity to FGFR inhibitors [51–53]. In our study, we found that LUSC had relatively higher frequency of FGFR3 alterations. FGFR3 fusion was detected in LUSC but not in LUAD, and FGFR3-TACC3 was found to be the most common fusion type. This fusion type was first described in GBM, then subsequently had been observed in various cancer types [54, 55]. TACC3 contained a dimerization domain that could lead to autophosphorylation and activation of FGFR3 signaling [56]. This fusion has been a therapeutic target of an FDA-approved drug, erdafitinib in BLCA, but its application in lung cancer still needs more clinical trials to explore. In addition to fusion, an S249C point mutation was also commonly detected in LUSC but not in LUAD. As described above, this mutation site was the FDA-recognized biomarker predictive of response to a pan-FGFR targeted inhibitor, erdafitinib in BLCA, but the clinical utility of targeted drugs in lung cancer with S249C mutation was still unknown.

Although FGFR3 alterations profile has been reported in several cancer types in previous studies [57], analysis results from these published data could be biased because of additional management during the publication processes. In this report, we profiled FGFR3 expression, methylation, alteration, and their prognostic and clinical implications across 32 TCGA cancer types which were mainly analyzed by the cBioPortal, this approach could unify the TCGA data from different cancer types by adopting ideally processed curation and unified clinical elements [58]. However, there were still some limitations that needed to be mentioned here. First of all, this study was a pan-cancer analysis of FGFR3 genetic alterations and lacked an in-depth investigation and analysis of individual cancer types. Moreover, the sample sizes of some tumor types from this study were not sufficient, and the full FGFR3 alteration spectrum was difficult to achieve in these cancer types. In addition, compared with the alteration frequency of other genes, like BRAF and EGFR, which had an alteration frequency of 8% and 7%, respectively, the frequency of FGFR3 genetic alterations (3%) across different cancer types was not that high which made our evaluation and analysis more challenging and difficult. Several key clues indicated in this study could provide the potential guidance and direction for future investigation.

CONCLUSIONS

In this study, we first reported the comprehensive pan-cancer profile of FGFR3 genetic alterations and their prognostic and clinical implications across various cancer types of TCGA which was covering over ten thousand tumor samples. Several FGFR3 alterations were more participated in the genesis and development of tumors, while other FGFR3 alterations more participated in targeted treatment. Some tumors with relatively low frequency of FGFR3 genetic alterations were correlated with patient prognosis, while other tumors with a relative high frequency of FGFR3 alterations were not. In conclusion, these analysis results provided a critical novel understanding of FGFR3 deregulation in tumor biology and identified potential therapeutic targets and prognostic indicators for some cancer types.

MATERIALS AND METHODS

Data acquisition and reanalysis using different bioinformatics tools

The Genotype-Tissue Expression (GTEx) database is an interactive web resource that collects transcriptome data of widely various tissue types from healthy individuals [59], allowing us to analyze FGFR3 expression in

normal tissues. The transcription levels of FGFR3 across different cancer types were extracted from cBioPortal [58, 60], and these transcription data were generated from normalized values with NormalizeExpressionLevels_allsampleref.py which represents the reference population of all samples independent of sample diploid status. All these transcription data of FGFR3 were log10 transformed finally. Then we explored the mRNA expression difference of FGFR3 between tumor tissues and their paired normal tissues across different cancer types or specific cancer subtypes of the TCGA project by using the "Gene_DE" module of TIMER2 (tumor immune estimation resource, version 2) approach. The log2 [TPM (Transcripts per million) +1] transformed expression data were applied for the box plots here. TIMER2 is a bioinformatics platform for systematical analysis of immune infiltrates across various tumor types [61]. For certain cancer types without normal tissues, we further used the GEPIA2 (Gene Expression Profiling Interactive Analysis, version 2) portal to investigate the FGFR3 mRNA expression difference between these tumors and corresponding normal tissues of the GTEx database. Moreover, the GEPIA2 portal also allowed us to further identify violin plots of the FGFR3 expression across different pathological stages of all TCGA cancer types. The log2 [TPM +1] transformed expression data were applied for the violin plots here. GEPIA2 is an interactive web server that analyzes RNA sequencing data from the GTEx and TCGA projects and allows users to conduct the differential expression analyses between tumor and normal tissues, the analysis of patient survival, as well as the access to the profiling of cancer type and pathologic stage, and so on [62]. Furthermore, the GSCALite platform is a comprehensive web server that provides various analysis types including drug sensitivity for genes analysis, genomic variations and their survival analysis, methylation analysis, and so on [63]. We used this platform to explore differential methylation of FGFR3 and downstream genes between tumor tissues and the adjacent normal tissues in different cancer types, and also the association between methylation and the expression of FGFR3 and downstream genes across various cancer types.

Kaplan-Meier Plotter is an online database that enables users to investigate patient survival across various cancer types of TCGA based on large sample datasets [64]. Herein, we used this plotter to analyze the correlation between FGFR3 mRNA expression and patient survival. Next, we downloaded the clinical data from cBioPortal to further identify the correlation between FGFR3 alteration and patient survival across different cancer types. We obtained the hazard ratio (HR), p-values, and the 95% confidence interval (CI),

then drew the forest plots to summarize these survival analyses.

cBioPortal is an open comprehensive platform that contains large-scale tumor genomics data and allows users to download and analyze multidimensional tumor genomics and clinical data [58]. In this study, we chose the "TCGA Pan Can Atlas Studies", and entered "FGFR3" for queries of the genetic alteration characteristics of FGFR3 across various cancer types. This pan-cancer study covered 10,953 patients and 10,967 samples across 32 TCGA cancer types (Supplementary Table 1). For the FGFR3 CNV data, the log ratio value represents: –2 = deep deletion; –1 = shallow deletion; 0 = diploid; 1 = gain; 2 = amplification. For the FGFR3 alteration data, a sample is defined as altered or unaltered (controls) for each gene according to the Onco Query Language (OQL) utilized in the query [37, 58].

Statistical analyses

The statistical analyses were analyzed with SPSS 12.0 software (IBM Analytics, United States). The statistic calculations on the Mutual Exclusivity tab are performed using all tumor samples from cBioPortal. Student's *t*-test, linear regression analysis, and Cox regression analysis were conducted when appropriate. $P < 0.05$ was defined as statistically significant if there was no special annotation. The main bioinformatics tools used in this study could be found in Supplementary Table 4.

Ethical statement

The authors are accountable for all aspects of the work in ensuring that questions related to the accuracy or integrity of any part of the work are appropriately investigated and resolved. None of the data have been previously published or appeared in copyrighted form elsewhere, and not previously published or unpublished data were cited in this paper. No ethics approval was required for this bioinformatics article, as it did not involve patients or patient data.

AUTHOR CONTRIBUTIONS

Conception and design: Yan YL and Xu ZJ. Writing, review, and/or revision of the manuscript: Li J, Hu K and Huang J. Administrative, technical, or material support: Zhou L. All authors approved final version of manuscript.

CONFLICTS OF INTEREST

The authors declare no conflicts of interest related to this study.

REFERENCES

1. Mossahebi-Mohammadi M, Quan M, Zhang JS, Li X. FGF Signaling Pathway: A Key Regulator of Stem Cell Pluripotency. Front Cell Dev Biol. 2020; 8:79.
https://doi.org/10.3389/fcell.2020.00079
PMID:32133359

2. Du J, Zhao Q, Liu K, Li Z, Fu F, Zhang K, Zhang H, Zheng M, Zhao Y, Zhang S. FGFR2/STAT3 Signaling Pathway Involves in the Development of MMTV-Related Spontaneous Breast Cancer in TA2 Mice. Front Oncol. 2020; 10:652.
https://doi.org/10.3389/fonc.2020.00652
PMID:32432040

3. Ou L, He X, Liu N, Song Y, Li J, Gao L, Huang X, Deng Z, Wang X, Lin S. Sialylation of FGFR1 by ST6Gal-I overexpression contributes to ovarian cancer cell migration and chemoresistance. Mol Med Rep. 2020; 21:1449–60.
https://doi.org/10.3892/mmr.2020.10951
PMID:32016470

4. Zhu M, Chen G, Yang Y, Yang J, Qin B, Gu L. miR-217-5p regulates myogenesis in skeletal muscle stem cells by targeting FGFR2. Mol Med Rep. 2020; 22:850–58.
https://doi.org/10.3892/mmr.2020.11133
PMID:32626929

5. Saborowski A, Lehmann U, Vogel A. FGFR inhibitors in cholangiocarcinoma: what's now and what's next? Ther Adv Med Oncol. 2020; 12:1758835920953293.
https://doi.org/10.1177/1758835920953293
PMID:32983265

6. Ledwon JK, Turin SY, Gosain AK, Topczewska JM. The expression of fgfr3 in the zebrafish head. Gene Expr Patterns. 2018; 29:32–38.
https://doi.org/10.1016/j.gep.2018.04.002
PMID:29630949

7. Wen X, Li X, Tang Y, Tang J, Zhou S, Xie Y, Guo J, Yang J, Du X, Su N, Chen L. Chondrocyte FGFR3 Regulates Bone Mass by Inhibiting Osteogenesis. J Biol Chem. 2016; 291:24912–21.
https://doi.org/10.1074/jbc.M116.730093
PMID:27729453

8. Li L, Zhang S, Li H, Chou H. FGFR3 promotes the growth and malignancy of melanoma by influencing EMT and the phosphorylation of ERK, AKT, and EGFR. BMC Cancer. 2019; 19:963.
https://doi.org/10.1186/s12885-019-6161-8
PMID:31619201

9. Guo P, Wang Y, Dai C, Tao C, Wu F, Xie X, Yu H, Zhu Q, Li J, Ye L, Yu F, Shan Y, Yu Z, et al. Ribosomal protein S15a promotes tumor angiogenesis via enhancing Wnt/β-catenin-induced FGF18 expression in hepatocellular carcinoma. Oncogene. 2018; 37:1220–36.
https://doi.org/10.1038/s41388-017-0017-y
PMID:29242604

10. Hayashi Y, Fujita K, Matsuzaki K, Eich ML, Tomiyama E, Matsushita M, Koh Y, Nakano K, Wang C, Ishizuya Y, Kato T, Hatano K, Kawashima A, et al. Clinical Significance of Hotspot Mutation Analysis of Urinary Cell-Free DNA in Urothelial Bladder Cancer. Front Oncol. 2020; 10:755.
https://doi.org/10.3389/fonc.2020.00755
PMID:32509577

11. Mansour H, Ouhajjou A, Bajic VB, Incitti R. Next-Generation Sequencing at High Sequencing Depth as a Tool to Study the Evolution of Metastasis Driven by Genetic Change Events of Lung Squamous Cell Carcinoma. Front Oncol. 2020; 10:1215.
https://doi.org/10.3389/fonc.2020.01215
PMID:32903616

12. Gelli E, Fallerini C, Valentino F, Giliberti A, Castiglione F, Laschi L, Palmieri M, Fabbiani A, Tita R, Mencarelli MA, Renieri A, Ariani F. *RB1* Germline Variant Predisposing to a Rare Ovarian Germ Cell Tumor: A Case Report. Front Oncol. 2020; 10:1467.
https://doi.org/10.3389/fonc.2020.01467
PMID:32974172

13. Shi MJ, Meng XY, Lamy P, Banday AR, Yang J, Moreno-Vega A, Chen CL, Dyrskjøt L, Bernard-Pirrot I, Prokunina-Olsson L, Radvanyi F. APOBEC-mediated Mutagenesis as a Likely Cause of FGFR3 S249C Mutation Over-representation in Bladder Cancer. Eur Urol. 2019; 76:9–13.
https://doi.org/10.1016/j.eururo.2019.03.032
PMID:30975452

14. Nadal R, Bellmunt J. Management of metastatic bladder cancer. Cancer Treat Rev. 2019; 76:10–21.
https://doi.org/10.1016/j.ctrv.2019.04.002
PMID:31030123

15. Qin Q, Patel V, Galsky MD. Urothelial carcinoma: the development of FGFR inhibitors in combination with

immune checkpoint inhibitors. Expert Rev Anticancer Ther. 2020; 20:503–12.
https://doi.org/10.1080/14737140.2020.1770600
PMID:32436413

16. Bansal P, Dwivedi DK, Hatwal D, Sharma P, Gupta V, Goyal S, Maithani M. Erdafitinib as a Novel and Advanced Treatment Strategy of Metastatic Urothelial Carcinoma. Anticancer Agents Med Chem. 2021. [Epub ahead of print].
https://doi.org/10.2174/1871520621666210121093852
PMID:33475078

17. Chell V, Balmanno K, Little AS, Wilson M, Andrews S, Blockley L, Hampson M, Gavine PR, Cook SJ. Tumour cell responses to new fibroblast growth factor receptor tyrosine kinase inhibitors and identification of a gatekeeper mutation in FGFR3 as a mechanism of acquired resistance. Oncogene. 2013; 32:3059–70.
https://doi.org/10.1038/onc.2012.319
PMID:22869148

18. Zehir A, Benayed R, Shah RH, Syed A, Middha S, Kim HR, Srinivasan P, Gao J, Chakravarty D, Devlin SM, Hellmann MD, Barron DA, Schram AM, et al. Mutational landscape of metastatic cancer revealed from prospective clinical sequencing of 10,000 patients. Nat Med. 2017; 23:703–13.
https://doi.org/10.1038/nm.4333
PMID:28481359

19. Helsten T, Elkin S, Arthur E, Tomson BN, Carter J, Kurzrock R. The FGFR Landscape in Cancer: Analysis of 4,853 Tumors by Next-Generation Sequencing. Clin Cancer Res. 2016; 22:259–67.
https://doi.org/10.1158/1078-0432.CCR-14-3212
PMID:26373574

20. Nakanishi Y, Akiyama N, Tsukaguchi T, Fujii T, Satoh Y, Ishii N, Aoki M. Mechanism of Oncogenic Signal Activation by the Novel Fusion Kinase FGFR3-BAIAP2L1. Mol Cancer Ther. 2015; 14:704–12.
https://doi.org/10.1158/1535-7163.MCT-14-0927-T
PMID:25589496

21. Williams SV, Hurst CD, Knowles MA. Oncogenic FGFR3 gene fusions in bladder cancer. Hum Mol Genet. 2013; 22:795–803.
https://doi.org/10.1093/hmg/dds486
PMID:23175443

22. Long X, Shi Y, Ye P, Guo J, Zhou Q, Tang Y. MicroRNA-99a Suppresses Breast Cancer Progression by Targeting FGFR3. Front Oncol. 2020; 9:1473.
https://doi.org/10.3389/fonc.2019.01473
PMID:32038996

23. Zhu G, Pei L, Li Y, Gou X. EP300 mutation is associated with tumor mutation burden and promotes antitumor immunity in bladder cancer patients. Aging (Albany NY). 2020; 12:2132–41.
https://doi.org/10.18632/aging.102728
PMID:32012118

24. Masser DR, Hadad N, Porter H, Stout MB, Unnikrishnan A, Stanford DR, Freeman WM. Analysis of DNA modifications in aging research. Geroscience. 2018; 40:11–29.
https://doi.org/10.1007/s11357-018-0005-3
PMID:29327208

25. Kim S, Wyckoff J, Morris AT, Succop A, Avery A, Duncan GE, Jazwinski SM. DNA methylation associated with healthy aging of elderly twins. Geroscience. 2018; 40:469–84.
https://doi.org/10.1007/s11357-018-0040-0
PMID:30136078

26. Qie Y, Wang L, Du E, Chen S, Lu C, Ding N, Yang K, Xu Y. TACC3 promotes prostate cancer cell proliferation and restrains primary cilium formation. Exp Cell Res. 2020; 390:111952.
https://doi.org/10.1016/j.yexcr.2020.111952
PMID:32156598

27. Tabernero J, Bahleda R, Dienstmann R, Infante JR, Mita A, Italiano A, Calvo E, Moreno V, Adamo B, Gazzah A, Zhong B, Platero SJ, Smit JW, et al. Phase I Dose-Escalation Study of JNJ-42756493, an Oral Pan-Fibroblast Growth Factor Receptor Inhibitor, in Patients With Advanced Solid Tumors. J Clin Oncol. 2015; 33:3401–08.
https://doi.org/10.1200/JCO.2014.60.7341
PMID:26324363

28. Loriot Y, Necchi A, Park SH, Garcia-Donas J, Huddart R, Burgess E, Fleming M, Rezazadeh A, Mellado B, Varlamov S, Joshi M, Duran I, Tagawa ST, et al, and BLC2001 Study Group. Erdafitinib in Locally Advanced or Metastatic Urothelial Carcinoma. N Engl J Med. 2019; 381:338–48.
https://doi.org/10.1056/NEJMoa1817323
PMID:31340094

29. Nogova L, Sequist LV, Perez Garcia JM, Andre F, Delord JP, Hidalgo M, Schellens JH, Cassier PA, Camidge DR, Schuler M, Vaishampayan U, Burris H, Tian GG, et al. Evaluation of BGJ398, a Fibroblast Growth Factor Receptor 1-3 Kinase Inhibitor, in Patients With Advanced Solid Tumors Harboring Genetic Alterations in Fibroblast Growth Factor Receptors: Results of a Global Phase I, Dose-Escalation and Dose-Expansion Study. J Clin Oncol. 2017; 35:157–65.
https://doi.org/10.1200/JCO.2016.67.2048
PMID:27870574

30. Lamont FR, Tomlinson DC, Cooper PA, Shnyder SD, Chester JD, Knowles MA. Small molecule FGF receptor inhibitors block FGFR-dependent urothelial
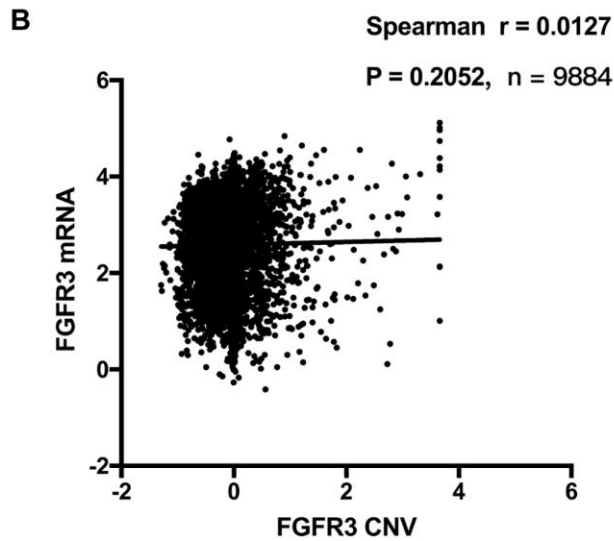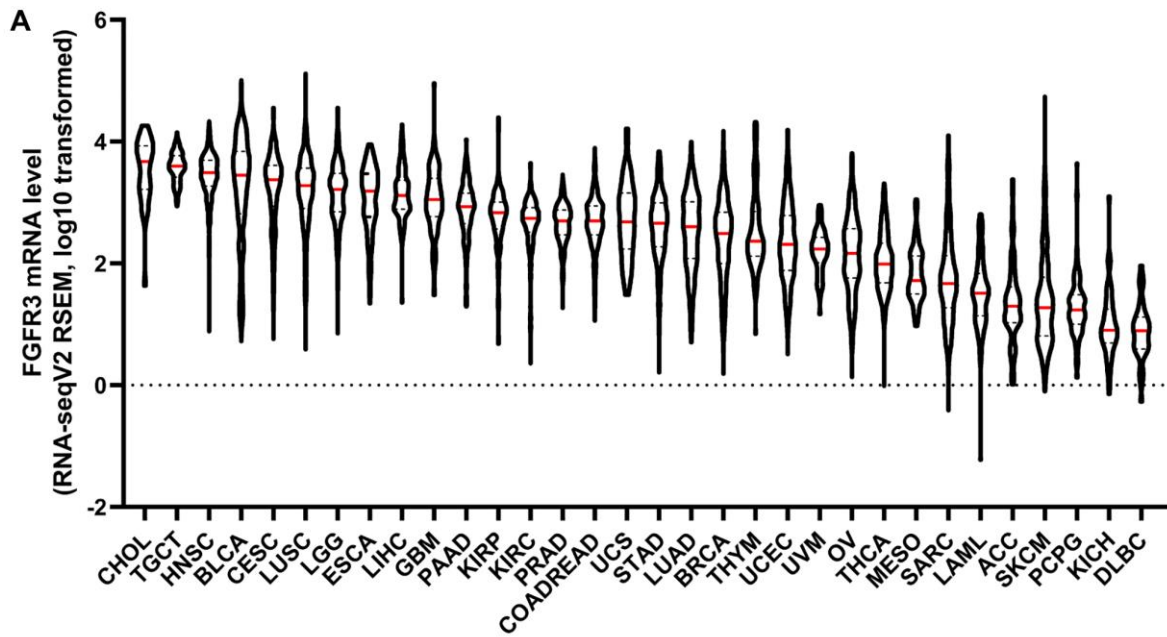
carcinoma growth *in vitro* and *in vivo*. Br J Cancer. 2011; 104:75–82.
https://doi.org/10.1038/sj.bjc.6606016
PMID:21119661

31. Bahleda R, Italiano A, Hierro C, Mita A, Cervantes A, Chan N, Awad M, Calvo E, Moreno V, Govindan R, Spira A, Gonzalez M, Zhong B, et al. Multicenter Phase I Study of Erdafitinib (JNJ-42756493), Oral Pan-Fibroblast Growth Factor Receptor Inhibitor, in Patients with Advanced or Refractory Solid Tumors. Clin Cancer Res. 2019; 25:4888–97.
https://doi.org/10.1158/1078-0432.CCR-18-3334
PMID:31088831

32. Pal SK, Rosenberg JE, Hoffman-Censits JH, Berger R, Quinn DI, Galsky MD, Wolf J, Dittrich C, Keam B, Delord JP, Schellens JHM, Gravis G, Medioni J, et al. Efficacy of BGJ398, a Fibroblast Growth Factor Receptor 1-3 Inhibitor, in Patients with Previously Treated Advanced Urothelial Carcinoma with *FGFR3* Alterations. Cancer Discov. 2018; 8:812–21.
https://doi.org/10.1158/2159-8290.CD-18-0229
PMID:29848605

33. Voss MH, Hierro C, Heist RS, Cleary JM, Meric-Bernstam F, Tabernero J, Janku F, Gandhi L, Iafrate AJ, Borger DR, Ishii N, Hu Y, Kirpicheva Y, et al. A Phase I, Open-Label, Multicenter, Dose-escalation Study of the Oral Selective FGFR Inhibitor Debio 1347 in Patients with Advanced Solid Tumors Harboring *FGFR* Gene Alterations. Clin Cancer Res. 2019; 25:2699–707.
https://doi.org/10.1158/1078-0432.CCR-18-1959
PMID:30745300

34. Nakanishi Y, Mizuno H, Sase H, Fujii T, Sakata K, Akiyama N, Aoki Y, Aoki M, Ishii N. ERK Signal Suppression and Sensitivity to CH5183284/Debio 1347, a Selective FGFR Inhibitor. Mol Cancer Ther. 2015; 14:2831–39.
https://doi.org/10.1158/1535-7163.MCT-15-0497
PMID:26438159

35. Nakanishi Y, Akiyama N, Tsukaguchi T, Fujii T, Sakata K, Sase H, Isobe T, Morikami K, Shindoh H, Mio T, Ebiike H, Taka N, Aoki Y, Ishii N. The fibroblast growth factor receptor genetic status as a potential predictor of the sensitivity to CH5183284/Debio 1347, a novel selective FGFR inhibitor. Mol Cancer Ther. 2014; 13:2547–58.
https://doi.org/10.1158/1535-7163.MCT-14-0248
PMID:25169980

36. Zhang J, Zhang L, Su X, Li M, Xie L, Malchers F, Fan S, Yin X, Xu Y, Liu K, Dong Z, Zhu G, Qian Z, et al. Translating the therapeutic potential of AZD4547 in FGFR1-amplified non-small cell lung cancer through the use of patient-derived tumor xenograft models. Clin Cancer Res. 2012; 18:6658–67.

https://doi.org/10.1158/1078-0432.CCR-12-2694
PMID:23082000

37. Gao J, Aksoy BA, Dogrusoz U, Dresdner G, Gross B, Sumer SO, Sun Y, Jacobsen A, Sinha R, Larsson E, Cerami E, Sander C, Schultz N. Integrative analysis of complex cancer genomics and clinical profiles using the cBioPortal. Sci Signal. 2013; 6:pl1.
https://doi.org/10.1126/scisignal.2004088
PMID:23550210

38. Cao J, Yang X, Li J, Wu H, Li P, Yao Z, Dong Z, Tian J. Screening and Identifying Immune-Related Cells and Genes in the Tumor Microenvironment of Bladder Urothelial Carcinoma: Based on TCGA Database and Bioinformatics. Front Oncol. 2020; 9:1533.
https://doi.org/10.3389/fonc.2019.01533
PMID:32010623

39. Na L, Bai Y, Sun Y, Wang Z, Wang W, Yuan L, Zhao C. Identification of 9-Core Immune-Related Genes in Bladder Urothelial Carcinoma Prognosis. Front Oncol. 2020; 10:1142.
https://doi.org/10.3389/fonc.2020.01142
PMID:32733809

40. Lyu L, Xiang W, Zheng F, Huang T, Feng Y, Yuan J, Zhang C. Significant Prognostic Value of the Autophagy-Related Gene P4HB in Bladder Urothelial Carcinoma. Front Oncol. 2020; 10:1613.
https://doi.org/10.3389/fonc.2020.01613
PMID:32903592

41. Roubal K, Myint ZW, Kolesar JM. Erdafitinib: A novel therapy for FGFR-mutated urothelial cancer. Am J Health Syst Pharm. 2020; 77:346–51.
https://doi.org/10.1093/ajhp/zxz329
PMID:32073123

42. Montazeri K, Bellmunt J. Erdafitinib for the treatment of metastatic bladder cancer. Expert Rev Clin Pharmacol. 2020; 13:1–6.
https://doi.org/10.1080/17512433.2020.1702025
PMID:31810398

43. Grünewald S, Politz O, Bender S, Héroult M, Lustig K, Thuss U, Kneip C, Kopitz C, Zopf D, Collin MP, Boemer U, Ince S, Ellinghaus P, et al. Rogaratinib: A potent and selective pan-FGFR inhibitor with broad antitumor activity in FGFR-overexpressing preclinical cancer models. Int J Cancer. 2019; 145:1346–57.
https://doi.org/10.1002/ijc.32224
PMID:30807645

44. Pal SK, Bajorin D, Dizman N, Hoffman-Censits J, Quinn DI, Petrylak DP, Galsky MD, Vaishampayan U, De Giorgi U, Gupta S, Burris HA, Soifer HS, Li G, et al. Infigratinib in upper tract urothelial carcinoma versus urothelial carcinoma of the bladder and its association with comprehensive

genomic profiling and/or cell-free DNA results. Cancer. 2020; 126:2597–606.
https://doi.org/10.1002/cncr.32806
PMID:32208524

45. Swanson SA, Robins JM, Miller M, Hernán MA. Selecting on treatment: a pervasive form of bias in instrumental variable analyses. Am J Epidemiol. 2015; 181:191–97.
https://doi.org/10.1093/aje/kwu284
PMID:25609096

46. Granberg KJ, Annala M, Lehtinen B, Kesseli J, Haapasalo J, Ruusuvuori P, Yli-Harja O, Visakorpi T, Haapasalo H, Nykter M, Zhang W. Strong FGFR3 staining is a marker for FGFR3 fusions in diffuse gliomas. Neuro Oncol. 2017; 19:1206–16.
https://doi.org/10.1093/neuonc/nox028
PMID:28379477

47. Frattini V, Pagnotta SM, Tala, Fan JJ, Russo MV, Lee SB, Garofano L, Zhang J, Shi P, Lewis G, Sanson H, Frederick V, Castano AM, et al. A metabolic function of FGFR3-TACC3 gene fusions in cancer. Nature. 2018; 553:222–27.
https://doi.org/10.1038/nature25171
PMID:29323298

48. He S, Ma X, Zheng N, Wang G, Wang M, Xia W, Yu D. PRDM14 mediates chemosensitivity and glycolysis in drug-resistant A549/cisplatin cells and their progenitor A549 human lung adenocarcinoma cells. Mol Med Rep. 2021; 23:149.
https://doi.org/10.3892/mmr.2020.11788
PMID:33355367

49. Wang X, Ren X, Liu W, Chen X, Wei J, Gong Z, Yan Y, Xu Z. Role of downregulated ADARB1 in lung squamous cell carcinoma. Mol Med Rep. 2020; 21:1517–26.
https://doi.org/10.3892/mmr.2020.10958
PMID:32016472

50. Chang C, Kong W, Mou X, Wang S. Investigating the correlation between DNA methylation and immune-associated genes of lung adenocarcinoma based on a competing endogenous RNA network. Mol Med Rep. 2020; 22:3173–82.
https://doi.org/10.3892/mmr.2020.11445
PMID:32945447

51. Wu YM, Su F, Kalyana-Sundaram S, Khazanov N, Ateeq B, Cao X, Lonigro RJ, Vats P, Wang R, Lin SF, Cheng AJ, Kunju LP, Siddiqui J, et al. Identification of targetable FGFR gene fusions in diverse cancers. Cancer Discov. 2013; 3:636–47.
https://doi.org/10.1158/2159-8290.CD-13-0050
PMID:23558953

52. Di Stefano AL, Fucci A, Frattini V, Labussiere M, Mokhtari K, Zoppoli P, Marie Y, Bruno A, Boisselier B, Giry M, Savatovsky J, Touat M, Belaid H, et al. Detection, Characterization, and Inhibition of FGFR-TACC Fusions in IDH Wild-type Glioma. Clin Cancer Res. 2015; 21:3307–17.
https://doi.org/10.1158/1078-0432.CCR-14-2199
PMID:25609060

53. Borad MJ, Champion MD, Egan JB, Liang WS, Fonseca R, Bryce AH, McCullough AE, Barrett MT, Hunt K, Patel MD, Young SW, Collins JM, Silva AC, et al. Integrated genomic characterization reveals novel, therapeutically relevant drug targets in FGFR and EGFR pathways in sporadic intrahepatic cholangiocarcinoma. PLoS Genet. 2014; 10:e1004135.
https://doi.org/10.1371/journal.pgen.1004135
PMID:24550739

54. Costa R, Carneiro BA, Taxter T, Tavora FA, Kalyan A, Pai SA, Chae YK, Giles FJ. FGFR3-TACC3 fusion in solid tumors: mini review. Oncotarget. 2016; 7:55924–38.
https://doi.org/10.18632/oncotarget.10482
PMID:27409839

55. Singh D, Chan JM, Zoppoli P, Niola F, Sullivan R, Castano A, Liu EM, Reichel J, Porrati P, Pellegatta S, Qiu K, Gao Z, Ceccarelli M, et al. Transforming fusions of FGFR and TACC genes in human glioblastoma. Science. 2012; 337:1231–35.
https://doi.org/10.1126/science.1220834
PMID:22837387

56. Gallo LH, Nelson KN, Meyer AN, Donoghue DJ. Functions of Fibroblast Growth Factor Receptors in cancer defined by novel translocations and mutations. Cytokine Growth Factor Rev. 2015; 26:425–49.
https://doi.org/10.1016/j.cytogfr.2015.03.003
PMID:26003532

57. Kacew A, Sweis RF. FGFR3 Alterations in the Era of Immunotherapy for Urothelial Bladder Cancer. Front Immunol. 2020; 11:575258.
https://doi.org/10.3389/fimmu.2020.575258
PMID:33224141

58. Cerami E, Gao J, Dogrusoz U, Gross BE, Sumer SO, Aksoy BA, Jacobsen A, Byrne CJ, Heuer ML, Larsson E, Antipin Y, Reva B, Goldberg AP, et al. The cBio cancer genomics portal: an open platform for exploring multidimensional cancer genomics data. Cancer Discov. 2012; 2:401–04.
https://doi.org/10.1158/2159-8290.CD-12-0095
PMID:22588877

59. Carithers LJ, Moore HM. The Genotype-Tissue Expression (GTEx) Project. Biopreserv Biobank. 2015; 13:307–08.
https://doi.org/10.1089/bio.2015.29031.hmm
PMID:26484569

60. Li J, Hu K, Zhou L, Huang J, Zeng S, Xu Z, Yan Y. Spectrum of Mesenchymal-Epithelial Transition Aberrations and Potential Clinical Implications: Insights From Integrative Pancancer Analysis. Front Oncol. 2020; 10:560615.
https://doi.org/10.3389/fonc.2020.560615
PMID:33178590

61. Li T, Fu J, Zeng Z, Cohen D, Li J, Chen Q, Li B, Liu XS. TIMER2.0 for analysis of tumor-infiltrating immune cells. Nucleic Acids Res. 2020; 48:W509–14.
https://doi.org/10.1093/nar/gkaa407
PMID:32442275

62. Tang Z, Kang B, Li C, Chen T, Zhang Z. GEPIA2: an enhanced web server for large-scale expression profiling and interactive analysis. Nucleic Acids Res. 2019; 47:W556–60.
https://doi.org/10.1093/nar/gkz430
PMID:31114875

63. Liu CJ, Hu FF, Xia MX, Han L, Zhang Q, Guo AY. GSCALite: a web server for gene set cancer analysis. Bioinformatics. 2018; 34:3771–72.
https://doi.org/10.1093/bioinformatics/bty411
PMID:29790900

64. Hou GX, Liu P, Yang J, Wen S. Mining expression and prognosis of topoisomerase isoforms in non-small-cell lung cancer by using Oncomine and Kaplan-Meier plotter. PLoS One. 2017; 12:e0174515.
https://doi.org/10.1371/journal.pone.0174515
PMID:28355294

Supplementary Figure 1. FGFR3 expression among 53 types of normal tissues.

Supplementary Figure 2. FGFR3 mRNA expression across different cancer types. (**A**) FGFR3 mRNA expression across all TCGA tumor types. RNA-seqV2 RSEM and log10 transformed were applied for log-scale. (**B**) The association between mRNA expression and linear CNV of FGFR3 across different tumors.
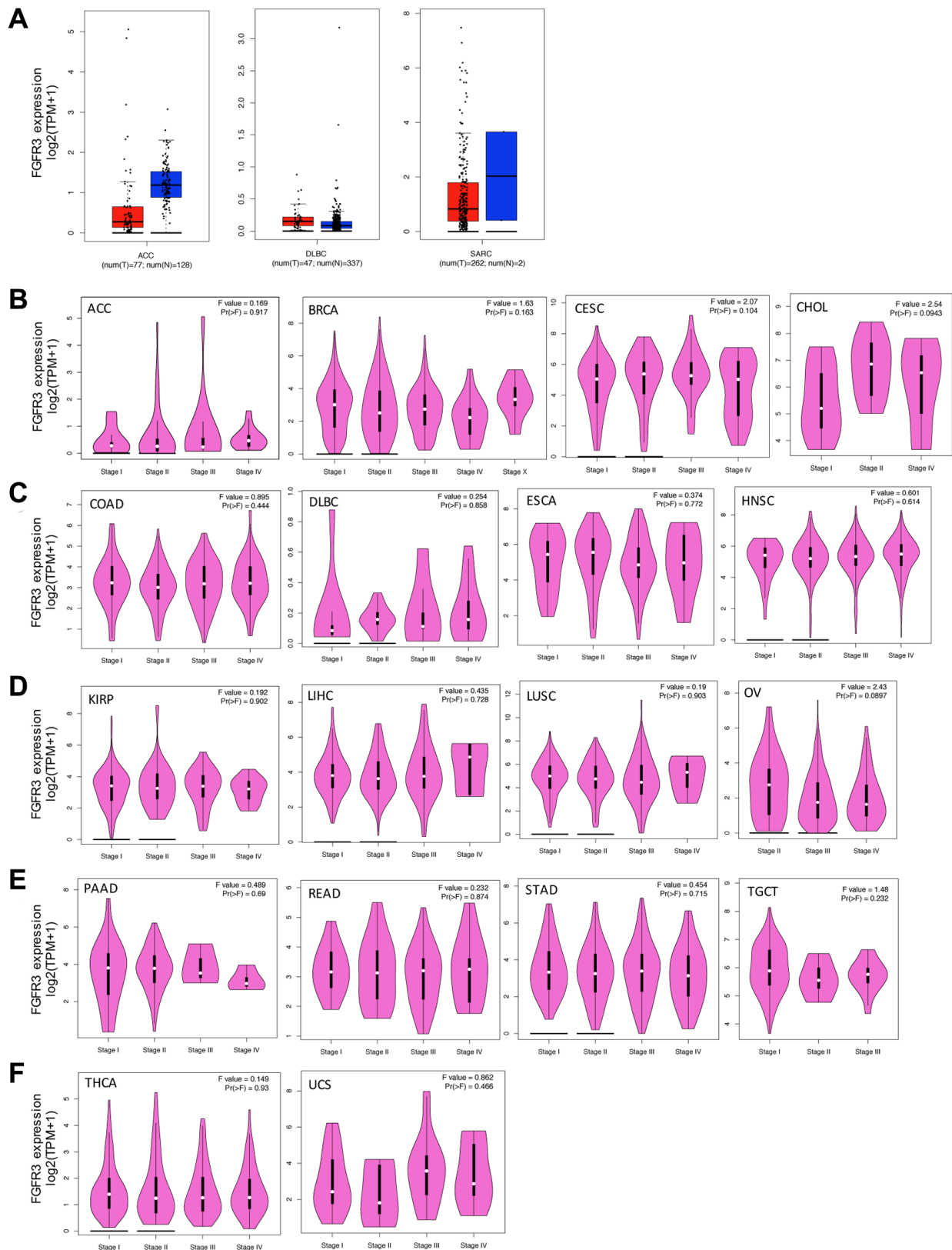
Supplementary Figure 3. FGFR3 mRNA expression in different cancer types and pathological stages. (**A**) The mRNA expression of FGFR3 in ACC, DLBC, and SARC in TCGA project were compared with the corresponding normal tissues of the GTEx database according to GEPIA2. (**B**–**F**) FGFR3 mRNA expression levels were analyzed by the main pathological stages of ACC, BRCA, CESC, CHOL, COAD, DLBC, ESCA, HNSC, KIRP, LIHC, LUSC, OV, PAAD, READ, STAD, TGCT, THCA, and UCS based on GEPIA2. The log2 (TPM +1) was applied for log-scale.
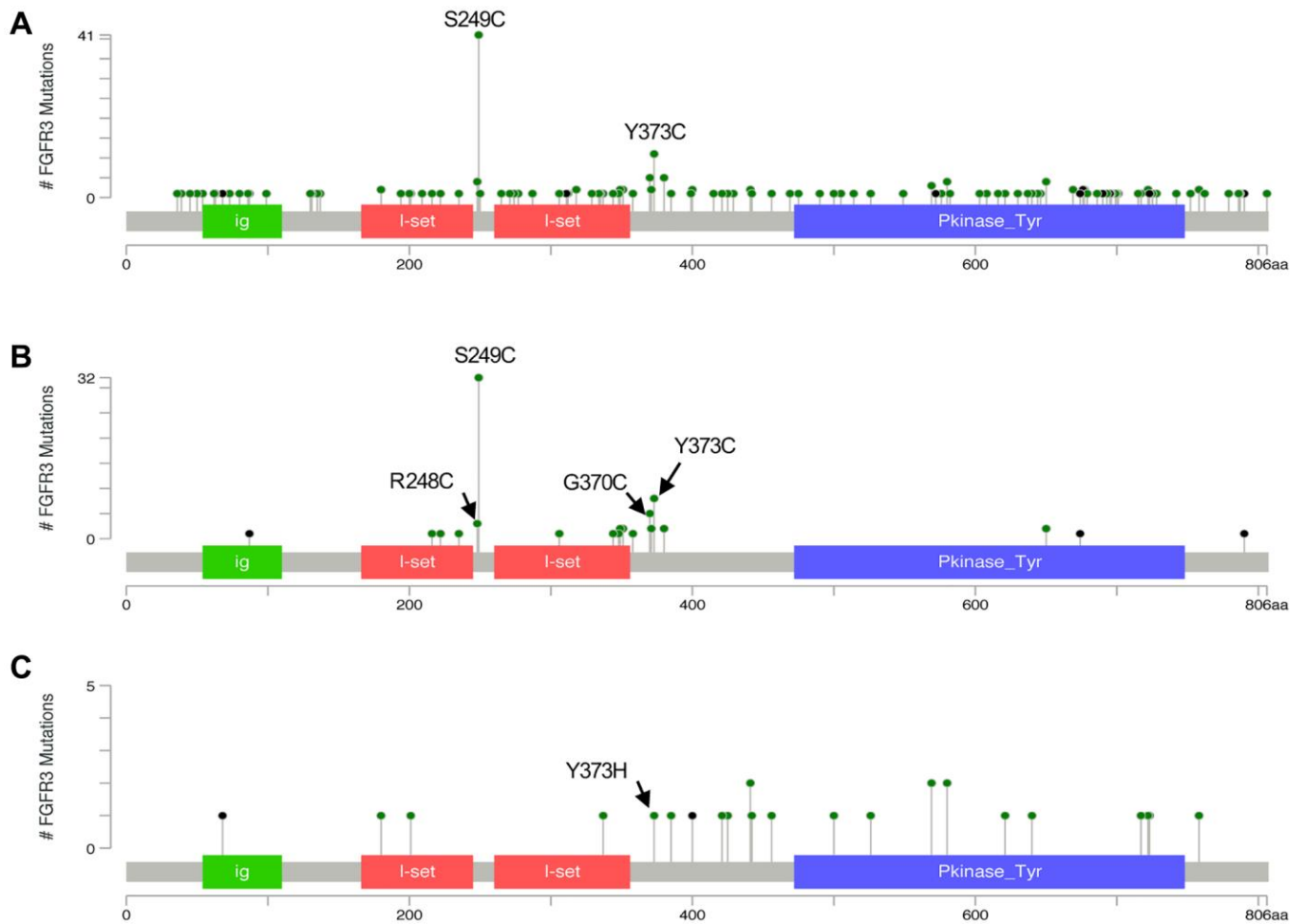
Supplementary Figure 4. FGFR3 mutation distribution in different functional domains. (**A**) FGFR3 mutation distribution in different FGFR3 functional domains in all TCGA tumor types. (**B**) FGFR3 mutation distribution in different FGFR3 functional domains in BLCA. (**C**) FGFR3 mutation distribution in different FGFR3 functional domains in UCEC.

	HR (95% CI)	*P*	n
BLCA	0.55 (0.21 – 1.43)	0.21	187
BRCA	0.67 (0.43 – 1.04)	0.072	947
CESC	0.50 (0.22 – 1.13)	0.088	174
ESCC	2.57 (0.97 – 6.77)	0.049	54
HNSC	0.41 (0.19 – 0.87)	0.017	124
KIRC	2.80 (0.63 – 12.46)	0.16	117
KIRP	2.63 (1.20 – 5.74)	0.012	183
LIHC	1.24 (0.84 – 1.82)	0.29	316
LUAD	0.70 (0.45 – 1.10)	0.12	330
LUSC	0.46 (0.27 – 0.76)	0.0019	300
OV	1.22 (0.82 – 1.83)	0.33	177
PAAC	0.57 (0.25 – 1.30)	0.18	67
COADREAD	0.40 (0.07 – 2.37)	0.30	47
SARC	1.70 (0.92 – 3.14)	0.089	152
STAD	0.56 (0.27 – 1.13)	0.10	215
TGCT	0.47 (0.18 – 1.25)	0.12	105
THCA	0.41 (0.16 – 1.02)	0.047	353
UCEC	1.84 (1.09 – 3.11)	0.022	422

Supplementary Figure 5. The correlation between FGFR3 expression and recurrence-free survival (RFS) as exhibited in forest plot based on Kaplan-Meier plotter.

Supplementary Tables

Supplementary Table 1. Summary of 32 TCGA tumor types and sample size.

TCGA Cancer Abbreviation	TCGA Cancer Type	Sample Number
ACC	Adrenocortical carcinoma	92
BLCA	Bladder urothelial carcinoma	411
BRCA	Breast invasive carcinoma	1084
CESC	Cervical squamous cell carcinoma and endocervical adenocarcinoma	297
CHOL	Cholangiocarcinoma	36
COADREAD	Colon adenocarcinoma/Rectum adenocarcinoma	594
DLBC	Lymphoid neoplasm diffuse large B-cell lymphoma	48
ESCA	Esophageal carcinoma	182
GBM	Glioblastoma multiforme	592
HNSC	Head and Neck squamous cell carcinoma	523
KICH	Kidney chromophobe	65
KIRC	Kidney renal clear cell carcinoma	512
KIRP	Kidney renal papillary cell carcinoma	283
LAML	Acute myeloid leukemia	200
LGG	Brain lower grade glioma	513
LIHC	Liver hepatocellular carcinoma	372
LUAD	Lung adenocarcinoma	566
LUSC	Lung squamous cell carcinoma	487
MESO	Mesothelioma	87
OV	Ovarian serous cystadenocarcinoma	585
PAAD	Pancreatic adenocarcinoma	184
PCPG	Pheochromocytoma and Paraganglioma	178
PRAD	Prostate adenocarcinoma	494
SARC	Sarcoma	255
SKCM	Skin cutaneous melanoma	448
STAD	Stomach adenocarcinoma	440
TGCT	Testicular germ cell tumors	149
THCA	Thyroid carcinoma	500
THYM	Thymoma	123
UCEC	Uterine corpus endometrial carcinoma	529
UCS	Uterine carcinosarcoma	57
UVM	Uveal Melanoma	80

Please browse Full Text version to see the data of Supplementary Table 2.

Supplementary Table 2. Detailed information about 234 FGFR3 somatic mutations from cBioPortal across 32 TCGA tumor types.

Supplementary Table 3. FGFR3 somatic mutation distribution in different protein functional domains for tumors with FGFR3 mutations and all tumors together.

	ig: Immunoglobulin domain (54-110aa)	I-set: Immunoglobulin I-set domain (166-245aa)	I-set: Immunoglobulin I-set domain (260-356aa)	Pkinase_Tyr: Protein tyrosine kinase (472-748aa)	Others	Fusion
Pan-cancer	9	9	20	54	100	42
BLCA	1	3	7	3	54	8
UCEC	1	2	1	11	9	
SKCM	5		2	10	4	1
COADREAD	1	3	1	8	5	
LUSC			1	1	7	7
HNSC			1	1	11	2
STAD	1		3	4	2	1
KIRP				4	3	2
LGG				1	1	5
CESC						6
GBM				3		3
PRAD			1	2		1
ESCA				1		2
LIHC		1				2
LUAD			1	1	1	
BRCA			1	1		
OV				1		1
PAAD			1	1		
KIRC				1		
LAML						1
MESO					1	
SARC					1	
UCS					1	

Supplementary Table 4. The main bioinformatics tools used to analyze the role of FGFR3 in pan-cancer.

Database	Samples	URL	References
cBioPortal	Tissues	http://cbioportal.org/	[58]
GTEx	Tissues	http://www.gtexportal.org/home/	[59]
TIMER2	Tissues	http://timer.cistrome.org/	[61]
GEPIA2	Tissues	http://gepia.cancer-pku.cn/	[62]
GSCALite	Tissues	http://bioinfo.life.hust.edu.cn/web/GSCALite/	[63]
Kaplan-Meier Plotter	Tissues	http://kmplot.com/	[64]